Institutionen för vattenbyggnad
Chalmers Tekniska Högskola

Department of Hydraulics
Chalmers University of Technology

ISSN 0348 - 1069

Calculated and Expected Thermal Ice Pressures in Five Swedish Lakes

by

Lars Bergdahl
Lars Wernersson

Report
Series B : 7

Göteborg 1978

Institutionen för vattenbyggnad
Chalmers Tekniska Högskola

Department of Hydraulics
Chalmers University of Technology

ISSN 0348 - 1069

Calculated and Expected Thermal Ice Pressures in Five Swedish Lakes

Lars Bergdahl

Lars Wernersson

Swedish Council for Building Research
Project No 75 0652-3

Report Göteborg 1977
Series B:7

Address: Institutionen för vattenbyggnad
Chalmers Tekniska Högskola
Fack
S-402 20 Göteborg, Sweden

Telephone: 031/81 01 00

SUMMARY

The temperature changes of land fast lake ice covers will give rise to loads against shores, dams or other structures. The magnitudes and recurrence of these thermal pressures are important in respect to the design.

A numerical model has been developed that calculates the thermal pressures in a lake ice cover for observed ice and snow cover characteristics and observed weather. The thermal diffusion in the ice is calculated by an implicit difference scheme. A complete energy budget is made for the ice or snow cover. The lateral expansion of the ice cover is supposed to be completely restricted, a constant coefficient of thermal expansion is adopted, and the deformation of the ice is supposed to be composed of a linear elastic element in series with a nonlinear creep element. The creep rate is set proportional to the stress to a power between 1 and 5 depending on the creep rate.

Those maxima of the calculated pressure that exceed 50 kN/m are listed as a time series for each lake, and the series is used to form an annual-maximum series and a peaks over a threshold series for the lake.

For five lakes in Sweden three types of probability distribution functions have been fitted to the series of annual maxima namely, the normal distribution, the lognormal distribution, and the double exponential distribution. Only the exponential distribution was fitted to the peaks over a threshold series. Because of the fact that weather observations are available on magnetic tape only for the last 12 to 16 years pressures could not be calculated for a longer period. This is not satisfactory for the estimation of events of recurrence intervals of a hundred to a thousand years. It gives, however, much better estimates than a single calculation for an intuitively chosen "extreme situation".

Reasonable estimates of the expected pressures of the return periods 100, 500, and 1000 years are given for the five lakes in the table below.

		Return Period (years)		
	Position	100	500	1000
Torne träsk	68.3°N 19.5°E	507	550	569
Stora Bygdeträsket	64.3°N 20.5°E	453	532	568
Runn	60.6°N 15.6°E	410	475	500
Glan	58.6°N 16.0°E	419	507	543
Vidöstern	57.1°N 14.0°E	330	380	400

Table Expected thermal ice pressures in kN/m for some return periods of annual maxima.

PREFACE

The late professor Lennart Rahm initiated ice engineering research at the Department of Hydraulics in 1968. Since 1969 the studies have been focused on the problem of thermal ice pressure against the walls of reservoirs. During the winters 69/70 and 70/71 field measurements of the course of temperature in an ice cover with and without snow were performed. The years 1972 to 1974 laboratory experiments were done in order to verify the mechanics of the thermal ice pressures.

The theoretical studies, which were roughly verified by the field and laboratory measurements, seem to show that it is possible to calculate thermal ice pressure rather accurately under given ambient conditions. So, if the weather, snow and ice thickness are given for a lake with steep shores, the ice pressure can be calculated. The methods of calculation are discussed in the report Thermal Ice Pressure in Lake Ice Covers (Bergdahl 1978) and other background material in Physics of Ice and Snow as Affects Thermal Ice Pressure (Bergdahl 1977).

The following study aims at an estimation of the design ice pressure in terms of periods of recurrence, or probability of extreme pressures. It has been performed on grants from the Swedish Council for Building Research and Chalmers University of Technology.

The authors wish to thank Mr Thomas Asp and Mr Bo Ekelund for their assistance as well as Mrs Göta Bengtsson and Mrs Ann-Marie Holmdahl for the typing, and Mrs Alicja Janiszewska for the drawing of the figures. We are grateful for the readiness of cooperation of the Ice and Climate Bureaus of the Swedish Meteorological and Hydrological Institute.

page

LIST OF CONTENTS

1. INTRODUCTION

When a land-fast ice cover has been formed on a lake or on a part of the sea, stresses and movements will arise in it because of temperature changes caused by the weather. The stresses will give rise to loads against shores, dams or other structures at the water course. It is a rather complicated matter to calculate these loads because of the unlinearity of the deformation of the ice, the complexity of ice covers, and the amount of weather information that is necessary. For an idealized description of the phenomenon of thermal ice pressure see paragraph 2.

The aim of this study is to be able to give the magnitude of expected thermal ice pressures on some lakes, distributed over Sweden to represent different climates. Therefore ice observations have been copied from handwritten notes and filed on computer for the selected lakes. The ice observations have in many cases been going on since January 1940. The weather records stretches even further back, but because of the amount of data for each day, only the years already on magnetic tape at SMHI could be used within the frame of the available time and money. The study is because of this limited to the years 1961 to 1976, which is a rather short time for estimating extreme events for structures usually designed for recurrence of events of 100 to 1000 years. For Torne träsk the available period was, unfortunately, only 1965 to 1976.

The methods of calculation are accounted for in this paper, but the choice of material properties and evaluations of alternative methods of calculation are not done. Information on these matters are given in two other reports (Bergdahl 1977, Bergdahl 1978).

2. THERMAL ICE PRESSURES

A very thin sheet of ice has a temperature close to $0^{o}C$. When such a sheet grows in thickness the temperature of its surface decreases due to the low air temperature. The upper layers of the ice contract but since the temperature at the lower boundary still is $0^{o}C$, the contraction causes tension, creep and cracks in the ice. The growth rate of the ice cover is mostly rather slow, so that, with the exception of the first few centimetres, the ice has time to creep without the formation of tensile cracks, that is, if the ice increases in thickness at a constant temperature of its upper surface.

If, however, at a time when the ice cover already has been formed and has increased in thickness at constant weather conditions, the air temperature suddenly falls considerably, the upper surface of the ice quickly assumes a new temperature of equilibrium, and after some time a new steady state gradient will be established in the ice cover. The upper surface will contract fast, but the lower boundary will keep its length since it is at the constant freezing-point temperature.

Now, the ice is floating on a horizontal water surface, and thus the free bending of the ice cover is restricted. Instead, the effect will be a bending moment in the ice cover, and the stresses will mostly be released in forming deep cracks, see Figure 2.1. If the change of temperature is very slow the ice may deform viscously without the formation of cracks.

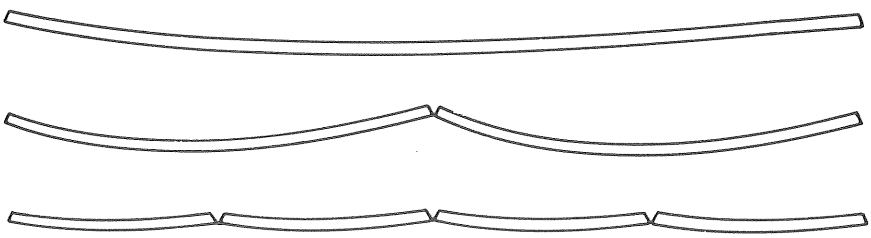

Figure 2.1 The bending and cracking of a floating ice cover due to a fast change of temperature in its upper surface.

The formation of the cracks is often sudden and is followed by a strong wave motion, which is felt if you are standing on the ice. You can also hear the cracks propagating across the ice cover, and it is clearly visible how they are spaced out at intervals of 10 to 20 m. Between these wide parallel cracks there is a system of thin surface cracks. The cracks will sooner or later be filled by water and drifting snow. Also cracks not extending all through the ice cover will partly be filled by snow and rime. The snow will be packed and recrystallized and the water will freeze in the slots. The freezing will sometimes cause pressure in the ice cover because of the increase of volume from water to ice. This pressure is, however, smaller than the extreme thermal pressures.

Later, if the ice cover is warmed due to mild weather, or water finding its way on to the ice, the upper layers will expand again. Depending on the steepness of the shores, the thickness of the ice and the rate of change of temperature, pressure will develop in the ice, and may be followed by a shove up onto a beach, or folding of the ice cover against banks and in zones of weakness, see Figure 2.2.

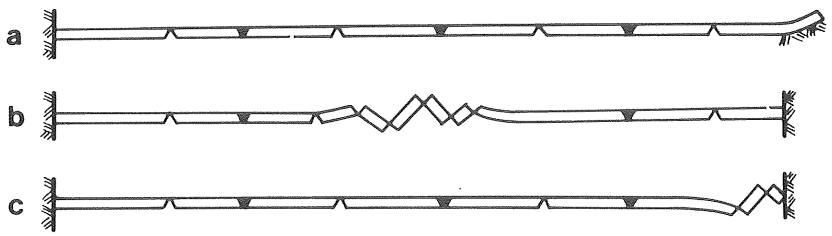

Figure 2.2 Examples of expanding ice covers

a) shoving up onto a beach
b) folding out on a lake
c) folding at a shore.

The magnitude of the ice pressure in the ice cover will be due to the rate of change of temperature in the ice, the coefficient of thermal expansion, the rheology of ice, the extent to which the cracks have been filled, the thickness of the ice cover, and the degree of restriction from the shores.

Of course, the rate of change of temperature in an ice cover depends on the change of weather conditions such as wind speed, air temperature, solar radiation, and the depth of the snow cover.

Expected magnitudes of ice pressures due to thermal expansion at a certain lake is thus obviously a function not only of ice and snow properties but also of the local climate, ice conditions and lake configuration.

3. PARTAKING PHYSICAL PROCESSES

A survey of the different processes considered when calculating ice pressures due to the thermal expansion of an ice cover is given below.

Thermal diffusion

Internal

The equation of thermal diffusion can be used to describe the rate of change of temperature within the ice if appropriate boundary conditions are given.

$$\frac{\partial \theta}{\partial t} = a \frac{\partial^2 \theta}{\partial x^2} + \frac{p(x, t)}{C_p \rho} \qquad \ldots (3.1)$$

where

t = time coordinate
x = vertical coordinate
θ = temperature at (x, t)
a = coefficient of thermal diffusion
C_p = specific heat capacity
ρ = bulk density
p = effect source per unit volume at (x, t).

$$a = \lambda / C_p \rho \qquad \ldots (3.2)$$

where λ = specific thermal conductivity.

External

Heat is convected away at the upper surface of the air, which simplified can be written

$$q = - A \Delta\theta \qquad \ldots (3.3)$$

where q = heat flow per unit area
A = coefficient of heat transfer
$\Delta\theta$ = temperature difference between the air and the ice surface.

The heat transfer also depends on the condensation or sublimation of ice on the surface. Radiation balance at the surface and the absorption of short-wave radiation within the ice will add to the external energy exchange. The long-wave radiation balance at the surface can simply be included by adding the balance to equation (3.3), whereas the short-wave energy flux must be included in equation (3.1) by for example,

$$p = k J \qquad \ldots (3.4)$$

where p = effect source per unit volume
k = absorption coefficient
J = is the intensity of short-wave radiation at the depth x.

A snow cover on the ice will change the external energy flux because of its low thermal conductivity and because of the change in radiation balance and its reflexion of short-wave radiation. Sometimes its weight will cause the ice-cover to sink below the water table, that is, the cover will be flooded with water.

Thermal expansion

Thermal expansion of ice is usually written

$$d\varepsilon = \alpha \cdot d\theta \qquad \ldots (3.5)$$

where $d\varepsilon$ = expansion per unit length caused by $d\theta$
α = linear coefficient of thermal expansion
$d\theta$ = temperature change

Sometimes it is easier to use the volume or length as functions of temperature directly, especially for saline ice where the expansion coefficient has singular points because of the crystallization of salts, while the volume always is finite.

Rheology

The mechanics of ice is very complicated and there are several ways of constructing mathematical models for the deformation. For each model the coefficients or moduli must then be evaluated from literature or experiments by curve fitting. A possible four-parameter model is for example,

$$\dot{\varepsilon} = \frac{1}{E}\dot{\sigma} + K D (\sigma/E)^n \qquad \ldots (3.6)$$

where $\dot{\varepsilon}$ = rate of deformation, $d\varepsilon/dt$

$\dot{\sigma}$ = stress rate, $d\sigma/dt$

E = modulus of elasticity

K, n = coefficients for viscous deformation

D = self diffusion coefficient for the molecules in ice

Nearly all parameters above are functions of ice type and temperature. The absorption coefficient and radiation balance are functions of wave-length too. The coefficient of heat transfer is a function of wind-speed and humidity.

The functions and coefficients used in this report will be specified for each process in its proper context below.

4. SELECTED LAKES

Five lakes with ice observations have been selected to represent different types of climate in Sweden. They should also have meteorological stations within reasonable distance. See Table 4.1 and the map of Figure 4.2 below for the approximate position of the lakes and their respective meteorological stations.

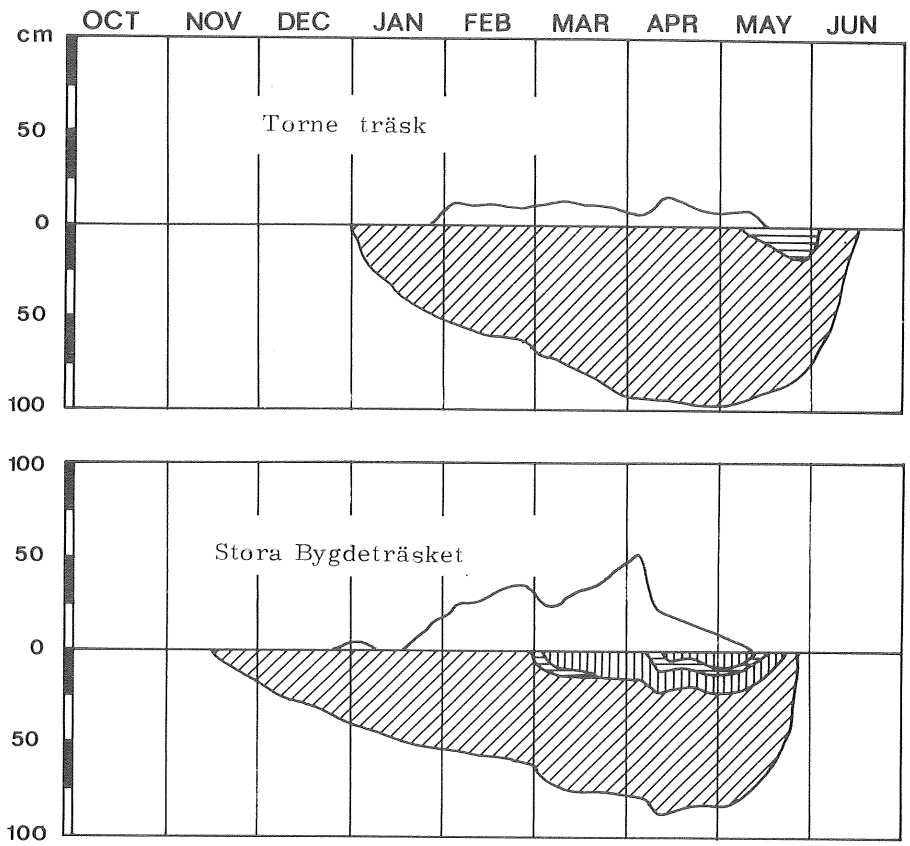

Figure 4.1 Depth of ice and snow the winter 1970/71.

snow
slush
snow ice
clear ice

Situation referred to water level

The northernmost lake Torne träsk is situated in a mountain area at 341 m above sea level. It regularly reaches an ice cover thickness of 1 m in late winter, and it is often free from snow. See Figure 4.1a. Stora Bygdeträsket lies in a forest area in the coast-land of northern Sweden, and has very often a complicated ice cover with layers of clear ice, snow slush, snow ice, and snow. See Figure 4.1b. The other selected lakes in central and southern Sweden have equally complicated ice covers as Stora Bygdeträsket, but the winters are shorter and more irregular. Glan and Vidöstern were, for example, nearly without ice in the winter 1972/73.

Table 4.1 Positions and altitudes for the five lakes and their weather stations.

	Latitude	Longitude	Area (km^2)	Altitude (m)
Lake Torne träsk	68.3°N	19.5°E	322	341
Station Kattuvuoma (1965-71)	68°17′N	19°54′E		355
Station Torne träsk (1971-76)	68°13′N	19°43′E		393
Lake Stora Bygdeträsket	64.3°N	20.5°E	29	131
Station Hällnäs-Lund	64°16′N	19°38′E		181
Lake Runn	60.6°N	15.6°E	68	106
Station Falun	60°37′N	15°38′E		122
Lake Glan	58.6°N	16.0°E	78	22
Station Norrköping	58°37′N	16°07′E		27
Lake Vidöstern	57.1°N	14.0° E	45	144
Station Hagshult	57°18′N	14°08′E		169

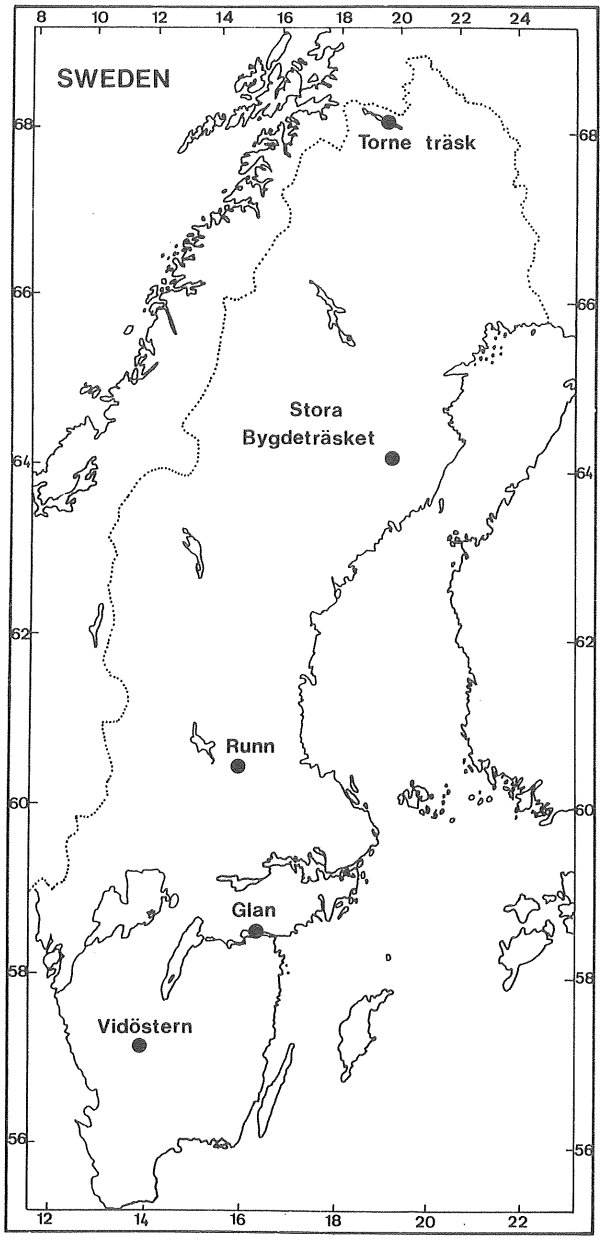

Figure 4.2 Positions of the selected lakes.

5. ENERGY BALANCE

The energy balance of ice or snow covers have mostly been studied in order to evaluate their growth or decay. Although such studies have often been performed with sophisticated methods, they work with daily, weekly or monthly mean values, why they can seldom be used directly for the calculation of the fast temperature fluctuations that are responsible for thermal ice pressure.

On the other hand, studies aiming at thermal ice pressures tend to oversimplify the energy balance of the surface by simply setting the surface temperature equal to the air temperature, or only calculating advective heat transfer. The short and long-wave radiation play, however, very important roles. The short-wave radiation increases the rate of change of temperature in the mornings, especially at clear weather. The long-wave back radiation can cause a considerable depression of the ice surface temperature, which is very pronounced by clear and calm weather. Omitting radiation therefore results in an underestimation of the daily temperature variations in an ice cover.

Below follows the terms of the energy fluxes according to the functions used in this study. For a discussion of these functions see Paily et al. (1974). The terms are the fluxes of

net solar radiation (+) (irradiation-reflexion)

long wave radiation from the atmosphere (+)

emitted long wave radiation (-)

heat transfer because of different temperature on the surface (sensible heat) and in the air (+ or -)

heat transfer due to moisture transport in the air and condensation (+, or sublimation -) on the surface (latent heat).

5.1 Heat Transport

Latent Heat

The convective heat transfer from the air to the surface consists of sensible heat, because of the temperature difference between the air and the surface, and latent heat, because of the vapour transport to the surface and condensation on it. The latent heat transfer is often written

$$q_e = f(u)\,(e_a - e) \qquad \ldots (5.1)$$

where e_a is the vapour pressure of the air 2 m above the surface

e the saturation vapour pressure on the ice surface

The saturation vapour pressure over an ice surface is a function of the surface temperature and is in this study approximated by a linear function

$$e = a\,(1 + b\,\theta); \quad -32^{o} \leqslant \theta \leqslant 0 \qquad \ldots (5.2)$$

where $a = 610$ Pa

$b = (32^{o}C)^{-1} = 0.031^{o}C^{-1}$

θ = the ice surface temperature.

The chosen wind function by Rymsha-Donichenko has been recommended by Paily et al. (1974)

$$f(u) = \rho L_s a\,(1 + bu + c\,(\theta - \theta_a)) \qquad \ldots (5.3)$$

where $a = 2.42 \cdot 10^{-11}$ m/s Pa

$b = 0.49$ s/m

$c = 4.36 \cdot 10^{-2}$ K^{-1}

$\rho = 1000$ kg/m^3 the density of water

$L_s = 2.84 \cdot 10^{6}$ J/kg the specific heat of sublimation (freezing + condensation)

u the wind speed at 2 m above the surface

θ the surface temperature

θ_a the air temperature at 2 m

Sensible Heat

The sensible heat transfer and the latent heat transfer is usually considered proportional to each other. The ratio between the two types of heat transfer is called Bowen's ratio

$$B = \gamma\,(\theta_a - \theta)/(e_a - e) \qquad \ldots (5.4)$$

where $\gamma = 61$ Pa/K is the psycrometric "constant".

The sensible heat transfer can now be written

$$q_S = B\, q_e = f(u)\ \gamma\ (\theta_a - \theta) \qquad \ldots (5.5)$$

where q_e is given by equation (5.1)
$f(u)$ - " - equation (5.3)
B - " - equation (5.4)

Finally the total convective heat transfer to the surface is written

$$q_c = q_e + q_S = f(u)\ \left[(e_a - e) + \gamma\ (\theta_a - \theta)\right] \qquad \ldots (5.6)$$

5.2 Radiation Fluxes

Emitted Long-Wave Radiation

The emitted long-wave radiation from the ice surface can be calculated by the Stefan-Boltzmann law of radiation with due respect to the emissivity of the ice or snow surface.

$$q_b = \varepsilon \cdot \sigma \cdot T^4 \qquad \ldots (5.7)$$

where $\sigma = 5.6697 \cdot 10^{-8}\ W/m^2K^4$
the Stefan-Boltzmann constant

T = the absolute temperature of the ice surface

ε = the emissivity of the surface.

In the calculations $\varepsilon = 0.97$ is used for both snow and ice.

The above expression must be linearized in order to make the system of equations linear and solvable by standard methods. The fourth-order binomial expansion of (5.7) for $T = A + \theta_s$ gives if two terms are considered:

$$q_b = \varepsilon \cdot \sigma \cdot (A^4 + 4A^3\, \theta_s) \qquad \ldots (5.7b)$$

where $A = 273.15$ K
θ_s = the temperature of the ice surface in ^oC.

Absorbed Long Wave Radiation

The atmosphere is also considered a gray body that emits radiation at the rate

$$q_{la} = \varepsilon_a \cdot \sigma \cdot T_a^4 \qquad \ldots (5.8)$$

where ε_a is the emissivity of the atmosphere
σ the Stefan-Boltzmann constant
T_a the absolute temperature of the air at 2 m above the surface

The emissivity of the atmosphere is a function of its content of water vapour. The relation set up by Ångström 1915 (See Paily et al. 1974) is used

$$\varepsilon_a = a - b \exp(-c\, e_a) \qquad \ldots (5.9)$$

where $a = 0.806$
$b = 0.236$
$c = 1.15 \cdot 10^{-3}\ \mathrm{Pa}^{-1}$
e_a is the water vapour pressure at 2 m above ground

The emission of the atmosphere is also influenced by the presence of cloud-covers. Approximately this can be taken into account by

$$q_{lc} = q_{la} (1 + k C^2) \qquad \ldots (5.9b)$$

where $k = 0.0027$
C the cloud cover in eighths

The absorbed long wave radiation flux from the atmosphere is finally

$$q_l = \varepsilon\, \varepsilon_a\, \sigma\, (1 + k C^2) \cdot T_a^4 \qquad \ldots (5.10)$$

where ε is the emissivity of the ice or snow surface, $\varepsilon = 0.97$.

Absorbed Solar Radiation

The incoming short wave radiation is supposed to be composed of the direct solar irradiction 0.9 kW/m^2, calculated on an area normal to the sun's rays, and diffuse sky radiation 0.1 kW/m^2. The flux through a horizontal surface from a clear sky is then written

$$q_{CL} = (a \cdot \sin \alpha + b) \quad \ldots (5.11)$$

where $a = 0.9\ kW/m^2$
$b = 0.1\ kW/m^2$
α is the altitude of the sun

The altitude of the sun is approximately set to

$$\alpha = \text{arc sin}\,(\sin \varphi \sin \delta + \cos \varphi \cos \delta \cos h) \quad \ldots (5.12)$$

where δ is the declination of the sun
φ the latitude
h local hour angle of the sun

The declination is written

$$\delta = 0.409 \cos((172 - D) \cdot 2\pi/365)\ \text{rad} \quad \ldots (5.13)$$

where D is the number of the day in a year with D = 1 for January 1.

The local hour angle of the sun

$$h = (H - a)\pi/a\ \text{rad} \quad \ldots (5.14)$$

where a = 12 h
H is the solar time of the day $0 \leqslant H < 24$ h

If the sun is below the horizon, that is, $\sin \alpha < 0$ the short wave radiation is set to zero $q_{CL} = 0$.

The solar radiation is reduced by cloud covers. Approximately it is written

$$q_C = q_{CL} (0.35 + 0.65 (1 - C/8)) \quad \ldots (5.15)$$

where q_{CL} is the radiation from a clear sky, equation (5.11)
C is the cloud cover in eighths

The function (5.15) is correct only for the mean value over a day, while the short term fluctuations are much greater when clouds intermittently pass the sun.

The incoming short wave radiation is supposed to be distributed in different wave-length bands so that 50 % of the energy flux lies between 350-700 µm, 25 % between 700-1200 µm, and 25 % between 1200-4000 µm.

Some of the incident light is reflected from the snow or ice cover. The absorbed radiation is for an optically rough surface (snow, snow ice, candled ice etc.) calculated according to

$$q_s = (1 - r) q_C \quad \ldots (5.16)$$

where q_C is the incident radiation equation (5.15)
r is the reflection coefficient (albedo)

In Table 5.1 below the used values for the reflection coefficients are given

Table 5.1 Coefficients of reflection for ice and snow surfaces used in the calculations

Wave-length band (µm)	Snow	Snow ice
350 - 700	0.9	0.05
700 - 1200	0.7	0.05
1200 - 4000	0.6	0.05

For clear ice the direct light is calculated as being reflected against a polished surface. If the angle of incidence is α_1 and the angle of refraction is β, the coefficient of reflection is calculated as

$$r = \frac{1}{2}\left[\frac{\sin^2(\alpha_1 - \beta)}{\sin^2(\alpha_1 + \beta)} + \frac{\tan^2(\alpha_1 - \beta)}{\tan^2(\alpha_1 + \beta)}\right] \quad \ldots (5.17)$$

where $\sin \alpha_1 = 1.31 \sin\beta$

$0 \leqslant \beta \leqslant \alpha_1$

$\alpha_1 = \pi/2 - \alpha$

α is the altitude of the sun.

See sketch Figure 5.1.

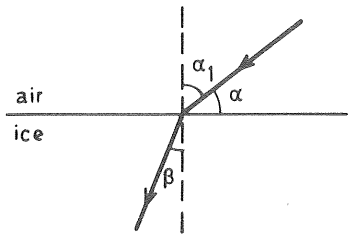

Figure 5.1 Definition sketch of angles.

For the diffuse light the coefficient is set to 0.02 and consequently the absorbed radiation flux is written

$$q_s = ((1 - r)\, a \sin\alpha + 0.98\, b) \cdot (0.35 + 0.65\,(1 - C/8)) \quad \ldots (5.18)$$

where $a = 0.9$ kW/m^2

$b = 0.1$ kW/m^2

C the cloud cover in eighths

r the reflexion coefficient according to equation (5.17)

Compare equations (5.11) and (5.15).

6. THERMAL DIFFUSION

The equation of thermal diffusion is used to describe the rate of change of temperature within the ice

$$\frac{\partial \theta}{\partial t} = a \frac{\partial^2 \theta}{\partial x^2} + \frac{p\,(x, t)}{C_p \rho} \qquad \ldots (6.1)$$

where t is the time
x the vertical coordinate
θ the temperature at (x, t)
a coefficient of thermal diffusion
C_p = 2120 J/kgK the specific heat capacity
ρ the bulk density
p the effect source per unit volume at (x, t)

$$a = \lambda / C_p \rho \qquad \ldots (6.2)$$

where λ is the specific thermal conductivity.

The bulk density ρ is given the following values

snow	250 kg/m^3
snow ice	890 kg/m^3
columnar ice	916, 8 kg/m^3

The thermal conductivity is set to the following constant values for the three used materials

snow	0, 3 W/mK
snow ice	2, 14 W/mK
columnar ice	2, 24 W/mK

The long-wave radiation and the heat transfer at the upper surface of the ice can be included in the source term p but can also be treated as a boundary condition. The short wave radiation must be separately considered as it is absorbed not only in the upper surface of the ice but throughout the thickness of the ice cover.

For an internal layer at the depth x from the upper surface of the ice the quantity p(x, t) is absorbed

$$p(x,t) = q_s k e^{-kx} \qquad \ldots (6.3)$$

where q_s is the solar radiation that penetrates into the ice, equation (5.16) or (5.18). q_s is a function of time.

t the time

x depth in the ice cover

k absorption coefficient

The used absorption coefficients for the three different materials and the three wave-length bands are given in the table below.

Table 6.1 Absorption coefficients $k(m^{-1})$ given for different wave-length bands

wave-length (μm)	350-700	700-1200	1200-4000
snow	120	200	10 000
snow ice	30	50	10 000
columnar ice	0,2	2	5 000

For the uppermost layer of the ice the source term is now written

$$p(0,t)\,dx = q_l - q_b + q_c + q_s k e^{-kx}\,dx \qquad \ldots (6.4)$$

where q_l is the absorbed long wave radiation from the atmosphere, equation (5.10)

q_c the total convective heat transfer to the surface, (equation 5.6)

q_b emitted long-wave radiation, equation (5.7)

At the lower boundary of the ice heat is supposed to be taken only from the freezing of water. The heat diffusion in the underlying water is thus neglected, and the source term at the lower boundary is written

$$p(h,t)\,dx = q_s\, k\, e^{-kx}\, dx + L\, \rho\, \frac{dh}{dt} \qquad \ldots (6.5)$$

where h is the thickness of the ice cover

$L = 3.34 \cdot 10^5$ J/kg is the specific heat of fusion

$\rho = 916.8$ kg/m^3 the density of ice

The equation of thermal diffusion is solved numerically with the help of an implicit difference method. The used scheme is described in paragraph 10.

7. EXPANSION AND DEFORMATION

7.1 Thermal Expansion of the Ice

The linear coefficient of thermal expansion is set constant, and the free expansion of the ice cover is written

$$d\varepsilon = \alpha \, d\theta \qquad \ldots (7.1)$$

where $\alpha = 4.82 \ 10^{-5}/K$ the linear coefficient of thermal expansion
$d\theta$ temperature increment
$d\varepsilon$ expansion increment per unit length caused by $d\theta$

7.2 Deformation of the Ice Cover

The thermal expansion of the ice cover is restricted by the shores of the ice. In the calculations the restriction is supposed to be complete so that the ice cover does not move horizontally at any point, that is, the thermal expansion and the deformation is supposed to be equal. The equation used for the deformation is

$$\dot{\varepsilon} = \frac{\dot{\sigma}}{E} + KD \, \sigma^n \qquad \ldots (7.2)$$

where $\dot{\varepsilon} = d\varepsilon/dt$ the rate of deformation eq. (7.1)
σ the horizontal stress in the ice
$\dot{\sigma} = d\sigma/dt$ the rate of change of stress
E the elastic modulus
$K = 4.40 \cdot 10^{-16} \ m^{-2} \ P_a^{-n}$
$n = 3.651$
$D =$ the coefficient of self diffusion of the molecules in ice.

$$E = (1 - c\,\theta) \cdot 6.1 \ GPa \qquad \ldots (7.3)$$

where $c = 0.012 \ ^oC^{-1}$

$$D = D_o \exp(-Q_s/RT) \qquad \ldots (7.4)$$

where D_o = $9.13 \cdot 10^{-4}$ m^2/s
Q_s = 59.8 kJ/mol the activation energy for self diffusion
R = 8.31 J/(mol K) the universal gas constant
T the absolute temperature

7.3 Pressure against the Shore and Buckling

The load per unit of length against the shore or the ice pressure (N/m) is calculated by integrating the stress over the depth of the ice cover. That is

$$P(t) = \int_0^h \sigma(x,t)\, dx \qquad \ldots (7.5)$$

where t and x are time and vertical coordinates respectively,
$\sigma(x,t)$ the stress calculated according to eq. (7.2)
h the depth of the ice cover
P (t) the thermal ice pressure

If the calculated ice pressure P is greater than the value for elastic buckling the value of P is set to that value and the event is listed in the print-out. The buckling load is hypothetically calculated to

$$P_b = 2\sqrt{\rho_w g\, E\, h^3/12\,(1-\nu^2)} \qquad \ldots (7.6)$$

where ρ_w = 1000 kg/m^3 is the density of water

g = 9.81 m/s^2 the earth acceleration

E the elastic modulus of the ice at mean depth of the ice cover, according to equation (7.3)

h the thickness of the ice

ν = 0 Poisson's modulus

8. WEATHER OBSERVATIONS

8.1 Received Data

The weather parameters that are used in the numerical model are

air temperature
extreme temperature of ditto
wind speed
cloud cover
air vapour pressure

Observations of these parameters have been supplied by SMHI (Swedish Meteorological and Hydrological Institute). The data was filed on magnetic tape for the concerned stations. The observations are performed at 0, 6, 12 and 18 GMT but for some stations there is no night observation performed. A specification for the different stations are given in the end of this chapter. The geographical position of the stations are given in table 4.1. First, however, a description of the used parameters will be given.

Air Temperature θ_a

The air temperature is given in degrees Celsius and is read on mercury thermometers graduated in fifth of a degree. The extreme temperatures are read on maximum and minimum thermometers graduated in half degrees. The latter are read and adjusted at 6 and 18 GMT at the concerned stations.

When the night temperature is not available the minimum temperature observed at 6 GMT is used instead. This is the minimum temperature of the preceding 12 hours, that is, since 18 GMT the day before. The minimum thermometers are checked regularly by comparing their readings with those of the mercury thermometer. From these readings a mean correction is obtained which is applied to all readings of the minimum temperature at the station.

Wind Speed u

At the stations the wind speed has been estimated according to the Beaufort scale. The wind velocities are the mean equivalents to the Beaufort scale.

Cloud Cover C

The cloud cover or cloudiness is given in octas, i.e. the figure indicate how many eighths of the sky are covered by clouds.

Air Vapour Pressure e_a

The humidity contents of the air are expressed by the vapour pressure. The humidity has been measured by hair hygrometers (Pernix-hair) at all included stations.

8.2 Modification of the Data

The received metoerological data is only given, at best, for every sixth hour (0, 6, 12, 18 GMT) during a period. The computational model works, however, with weather data for every calculation step, in this case for every hour. For points of time between observations linear interpolation is performed.

Linear Interpolation

The weather data is, for every hour, obtained through linear interpolation between the two sets of observational data. This is generally true for the data on wind and cloud cover and for almost all air vapour pressure data.

If the air vapour pressure is missing, it is assumed to be 300 Pa (3.0 mb) and is calculated exactly as if it had been an originally observed value.

Concerning the air temperature linear interpolation is performed if we have observations for four times a day (with extreme temperature) or three times a day without extreme temperature.

Special Linear Interpolation

If the air temperature is read three times a day, and the extreme minimum temperature is read at 6 GMT, too, a special linear interpolation is performed for interpolation during the night between 18 and 6 GMT. The minimum temperature observed at 6 GMT in the morning is used instead of the 0 GMT temperature. The temperature is, however, not assumed to occur at "midnight" but at a point of time at which the minimum temperature usually occurs according to the mean course of temperature at the latitudes concerned. The chosen points of time for the minimum temperature are listed in Table 8.1 below. The points of time have been chosen with the help of diagrams published in Klimatdata för Sverige (Taesler 1972).

Table 8.1 Assumed time (GMT) for the occurrence of the minimum temperatures for the lakes (stations). For local time, add 1 hour.

Lake (Station)	Month			
	Nov-March	April	May	June
Torne träsk (Torne träsk Kattuvuoma)	4	3	2	2
Stora Bygdeträsket (Hällnäs-Lund)	5	3	2	2
Runn (Falun)	6	4	3	2
Glan (Norrköping)	6	4	3	2
Vidöstern (Hagshult)	6	4	3	2

Table 8.2 Stations for observations of meteorological parameters. Remarks of limitation of the received data. The data is given for three/four times a day ((0), 6, 12, 18 GMT) if no remarks.

Station	Observation			Remark
	3 times/day without extreme temperature	3 times/day with extreme temperature	4 times/day with extreme temperature	
Kattuvuoma			650101 - 710630	
Torne Träsk		711101 -760630		
Hällnäs-Lund	610101 - 641130			Dec 1964 missing
			650101 - 760630	
Falun	610101 - 641231			
		650101 - 760630		
Norrköping	610101 - 641231			
			650101 - 760630	
Hagshult	610101 - 641231			
		700101 - 700131 (Jan 1970)	650101 - 691231	
		710401 - 710430 (April 1971)	700201 - 710831	
			710501 - 760630	

3 times/day observed at 6, 12, 18 GMT
4 times/day - " - 0, 6, 12, 18 GMT

9. ICE OBSERVATIONS

9.1 Description of Available Data

The ice and snow cover on some lakes in Sweden are reported once a week to SMHI. This has been done since January 1940. The instruction for the observations reads as follows:

"The measuring of the ice shall be performed where the thickness of the ice can be supposed to be representative. The hole must therefore be bored at least 50 m off the shore and at an assuring distance from the mouth of streams and the outlet. The measuring shall be performed once a week, and for each time a new hole shall be bored at a distance from the former ones".

On the paper form for the observations the thickness of the different layers of the ice cover is given from top to bottom. Other information on the form is notations, whether the snow cover is even, if there is snow slush all over the lake, if there are leads in the ice cover etc. For the calculations in this report only the thicknesses of the different layers are used. The ice cover is supposed to be quite even over the whole lake. An example of observation is given below from Stora Bygdeträsket.

Table 9.1 Ice thickness observation (cm) from Stora Bygdeträsket

	March 12	March 18	March 26	April 9 1976
snow	26	23	26	17
snow slush	4	-	-	-
snow ice		8	-	-
snow slush		3	-	-
snow ice		-	-	-
snow slush		-	-	-
snow ice		-	14	16
columnar ice	57	57	57	53

The selected lakes are listed in table 4.1. The ice observations have been filed on magnetic tape with the help of the criteria stated in para-

graph 9.2. For all the lakes the observations have been performed once a week since January 1940 except for Lake Vidöstern which has been observed every fortnight since November 1954, only.

9.2 Selection of Relevant Ice Data

The ice observations are filed at SMHI on the original forms only. For the purpose of the calculation of the ice pressures only relevant data has been copied to magnetic tape. The criteria for selection are:

1) Periods with a snow depth greater than 15 cm are omitted. Such deep layers of snow are supposed to insulate the underlying ice effectively from the weather fluctuations.

2) Layers below snow slush are not filed either, as these layers are at constant freezing point temperature till the snow slush has frozen to snow ice. Periods with snow slush directly under the snow cover are omitted.

3) The depth of the ice cover is supposed to be 1 cm when the ice is reported to have formed on the lake, but the observer has not been able to walk on it.

10. COMPUTER PROGRAMME

The thermal pressures and deformations of the ice is calculated with the help of a computer programme, where first the temperatures are solved by the use of an implicit difference scheme, thereafter pressures are calculated by an iteration of the deformation equation.

Before these calculations can be done it is, however, necessary to precondition the weather and ice input. Because the calculation of the energy exchange involves a lot of parameters, and because the ice cover is often rather complex, the programme is to a great extent administrating the terms of the system of equations and the interval limits in the ice.

The programme thus starts by reading the ice and weather input and preconditions them to fit into the system of equations. Thereafter follows an analysis of the radiation terms and an arrangement of the matrix-elements in the equation of diffusion. The temperatures are solved and the ice pressure is calculated. Finally the growth of the ice is calculated.

After this cycle of calculation the thickness of the bottom element is adjusted if necessary, new weather input is read and administrated for every six hour, or if a week has passed new ice conditions are read, and the temperature and pressure calculations are repeated from an appropriate stage of the programme.

Below follows a description of the most important manipulations in the programme.

10.1 Preconditioning of Input

In the initial phase of the computer programme the ice observation for the selected start time is read as well as the connected weather observation.

Ice Observations

If a layer of candled ice is registered it is assumed to be equivalent to columnar ice. The thickness of the candled ice is added to that of the columnar ice. This simplification will result in an overestimation of the ice pressure.

If snow slush exists calculations is performed only on layers situated above the snow slush, that is, snow and snow ice. The snow slush, which is a mixture of snow and water, has the temperature $0^{o}C$ and shields the layers underneath from temperature variations.

The cover as defined above is then divided into intervals with a closer division near the surface. The rate of change of temperature is greatest at the surface, and correct surface temperatures are important for calculating the heat transfer and long-wave back radiation. Coordinates are assigned to the limits of the different intervals starting with x = 0 m for the upper interface followed by 0.005, 0.015, 0.025, 0.050, 0.100, 0.150 m .... and so on for every fifth cm if there is no new material interface.

Example 1: 0.12 m columnar ice
x = 0.000, 0.005, 0.015, 0.025, 0.050, 0.100, 0.120.

Example 2: 0.12 m snow and 0.12 m columnar ice
x = 0.000, 0.005, 0.015, 0.025, 0.050, 0.100, 0.120, 0.170, 0.220, 0.240.

For each time-step ice growth is added to the lowest interval, and if the thickness of the lower element exceeds 55 mm it is divided into two elements the upper of which is assigned the thickness 50 mm. The temperatures in the two new elements are interpolated between the old points.

Weather observations

With respect to the time scale of the considered process and due to stability problems when calculating the unlinear deformation, a time step of one hour has proved to be reasonable. As mentioned earlier the weather observations are performed at 6 to 12 hours´ interval, why linear interpolation is used for the intermediate points of time. Compare paragraph 8.2.

Initial Temperature and Stress Distribution

The stress is set to zero at the reading of a new ice observation. The ice observation is entered at 18 GMT in order not to interfere with possible maximum pressure during the afternoon.

The initial temperatures are also recalculated for every new ice observation and consequent new division into ice intervals. This is done by first assigning a linear temperature profile with zero temperature at the lower boundary and the air temperature at the upper surface. Then the steady state solution is calculated by repeating the temperature calculations nine times ($\sim$ 9 h) for constant ambient conditions.

10.2 Temperature Calculation

Type of Scheme

The temperatures in the ice cover are calculated by the help of an implicit difference scheme (Crank-Nicholson). The implicit scheme was chosen so as to be able to make a rather free internal division into intervals, as this scheme gives unconditionally stable calculations for the internal points. The boundary conditions at the upper surface introduced instability, however, which was overcome by giving more weight to the later timestep. The weight given is $\beta = 0.6$.

The equation of diffusion

$$\frac{\partial \theta}{\partial t} = a \frac{\partial^2 \theta}{\partial x^2} \qquad \ldots (10.1)$$

is fundamentally approximated by the difference equation

$$\theta(x, t + \Delta t) = \theta(x, t) +$$

$$+ \frac{a}{2} \frac{\Delta t}{\Delta x^2} \left[(1 - \beta) \left\{ \theta(x + \Delta x, t) - 2\theta(x, t) + \theta(x - \Delta x, t) \right\} + \right.$$

$$\left. + \beta \left\{ \theta(x + \Delta x, t + \Delta t) - 2\theta(x, t + \Delta t) + \theta(x - \Delta x, t + \Delta t) \right\} \right] \quad \ldots \quad (10.2)$$

where the searched temperature $\theta(x, t + \Delta t)$ is a function of known temperatures at the point of time, t, and of unknown temperatures in the neighbour points, $x + \Delta x$ and $x - \Delta x$, at $t + \Delta t$. The equation (10.2) must thus be solved for all points in the ice simultaneously and this is done by a double sweep method.

Formulation of Equations

The diffusion equation to be considered has not the simple form (10.1) but contains also a source term, p, due to short wave radiation in internal points, as well as boundary conditions for the uppermost element. This was formulated in chapter 6 by $\partial\theta/\partial t = a\ \partial^2\theta/\partial t^2 + p(x, t)/C_p\rho$, and this equation is transcribed into a difference form which will be explained below. For convenience the time average $(1 - \beta)\ \theta(x, t) + \beta\ \theta(x, t + \Delta t)$ is denoted by $\bar{\theta}_i$ below where $i = 1$ denotes $x_1 = 0$ and $i = 2$, $x_2 = x_1 + \Delta x_1$ etc.

Upper Interface

The implicit scheme made it convenient to split the source term p into one part containing terms depending on the temperature of the ice surface $\bar{q}$ and another part with terms entirely dependent on the ambient conditions $\bar{\alpha}$.

$\bar{q}$ contains for the uppermost element

- longwave back-radiation: $\bar{q}_b$ (Eq. 5.7b)
- part of the total convective heat transfer:
  $f(\bar{u})(-\bar{e} - \gamma\bar{\theta})$ (Eq. 5.6)

$\bar{\alpha}$ contains for the uppermost element

- absorbed long-wave radiation:
  $\bar{q}_l$ (Expanded Eq. 5.10)
- absorbed short wave radiation: $\bar{q}_s\, k\Delta x$ (Eq. 6.3)
- part of the total convective heat transfer:
  $f(\bar{u})(\bar{e}_a + \gamma\bar{\theta}_a)$ (Eq. 5.6)

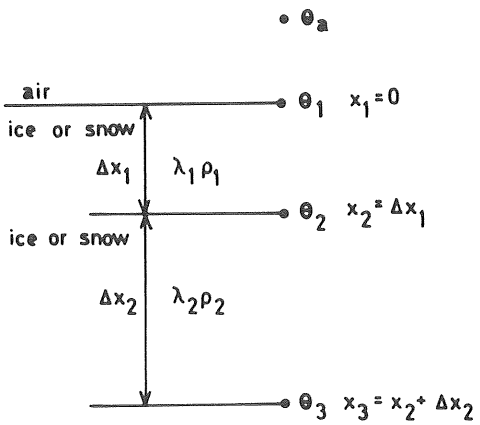

Figure 10.1 Definition sketch for difference scheme.

The difference formulation for the uppermost element with the thickness Δx_1 can now be written

$$\frac{\Delta\theta_1}{\Delta t} \cdot C_p \rho \frac{\Delta x_1}{2} = \frac{\lambda_1}{\Delta x_1}(\bar{\theta}_2 - \bar{\theta}_1) + \bar{q} + \bar{\alpha} \qquad \ldots (10.3)$$

where bars denote the weighted time average and $\Delta\theta_1 = \theta_1(t+\Delta t) - \theta_1(t)$.

Internal Points

The ice cover is composed of different materials, snow, snow ice and columnar ice. This is automatically concidered by the programme by writing the difference equation in a form that assumes the material interface case as the general one.

The diffusion equation for the internal points is written

$$\frac{\Delta\theta_i}{\Delta t} \frac{C_p}{2} (\rho_{i-1} \Delta x_{i-1} + \rho_i \Delta x_i) =$$

$$\frac{\lambda_{i-1}}{\Delta x_{i-1}} (\bar{\theta}_{i-1} - \bar{\theta}_i) + \frac{\lambda_i}{\Delta x_i} (\bar{\theta}_{i+1} - \bar{\theta}_i) +$$

$$+ \bar{\alpha}_{i-1/2} - \bar{\alpha}_{i+1/2} \qquad \ldots (10.4)$$

where $\bar{\alpha}_{i-1/2} - \bar{\alpha}_{i+1/2}$ is short-wave radiation absorbed in the neighbourhood of x_i. (Long-wave radiation and convective heat transfer influences only the surface element).

Lower Interface

At the ice-water or ice-slush interface the boundary condition $\theta = 0\,^{o}C$ is used. The heat conducted away from the boundary is after each time step used to estimate the ice growth at the boundary. The right hand side of equation (10.4) will give the ice growth Δx_x.

$$\Delta x_x \cdot \frac{\rho_{i-1} L}{\Delta t} = \frac{\lambda_{i-1}}{\Delta x_{i-1}} \bar{\theta}_{i-1} + \bar{\alpha}_{i-1/2} - \bar{\alpha}_i \qquad \ldots (10.5)$$

where L is the specific heat of fusion and ρ_{i-1} the density of the fused ice.

A limitation of the programme is that melting never can occur, as melting is not allowed in the inner points, but the temperature there is never allowed to rise over $0^{o}C$. A further consequence of this is that melting does not occur at the lower boundary either. This makes the programme no good for ice growth calculations. For ice-pressure calculations the simplification gives an overestimation of pressures, as the ice is considered dry in the calculations at a start of a cold period.

System of Equations

The system of equations that develops, when the equations (10.3) and (10.4) are gathered for all elements, is of the type

$$AT_2 = BT_1 + D \qquad \ldots (10.6)$$

where A and B are tridiagonal matrices

T_2 the column vector of new (unknown) temperatures $\theta_i(t+\Delta t)$, $i=1,2 \ldots .$

T_1 the column vector of old (known) temperatures $\theta_i(t)$, $i = 1,2 \ldots .$

D vector of terms that do not depend on ice temperatures ($\bar{\alpha}_i$)

The right hand side of Equation (10.6) consists of known quantities only why $C = BT_1 + D$ can be calculated and finally the double sweep method gives the solution:

$$T_2 = A^{-1} C \qquad \ldots (10.7)$$

Notes on Accuracy and Stability

The accuracy of the used scheme can for internal points be estimated by expansion in Taylor series. If first β is neglected it is found that the difference approximation of the right hand side of the equation of thermal diffusion (10.1) has a truncation error of

$$\Delta x^2/12 \cdot \partial^4\theta/\partial x^4 + O(\Delta x^4) \qquad \ldots (10.8)$$

and the approximation of the left hand side has a truncation error of

$$\Delta t/2 \cdot \partial^2\theta/\partial x^2 + O(\Delta t^2) \qquad \ldots (10.9)$$

The errors due to $\beta > 0.5$ is also of the same order as (10.9).

It can be shown by the von Neuman criterion that the used implicit scheme is unconditionally stable for all choices of length and time intervals. It proved, however, to be necessary to put slightly more weight ($\beta = 0.6$) on the later time step because of problems introduced at the upper boundary.

10.3 Pressure Calculations

The calculated temperature profile is used to calculate the thermal ice pressure for each interval separately. The pressures are then integrated over the depth of the ice which gives the total ice pressure (N/m).

Combining equations (7.1) and (7.2) gives

$$\alpha \frac{d\theta}{dt} = \frac{\dot{\sigma}}{E} + KD\ \sigma^n \qquad \ldots (10.10)$$

which is written

$$d\varepsilon = (\dot{\sigma}/E + KD\ \sigma^n)\, dt \qquad \ldots (10.11)$$

For each time step the left hand side can be approximated by the known quantity, $\Delta\varepsilon = \alpha\,\Delta\theta$.

Because the deformation equation is unlinear, a special iterative procedure is used to solve it. The equation is written on the form

$$\sigma_{k+1}^{\text{new}} = \sigma_k + E_m \left\{ \Delta\varepsilon - D_k K\ \sigma_k^n + D_{k+1} K\ \sigma_{k+1}^{n\ \text{old}} \right) \frac{\Delta t}{2} \Bigg\} \qquad \ldots (10.12)$$

where σ_k is the stress at the point of time $t = k\Delta t$

σ_{k+1} - " - at $t + \Delta t = (k+1)\,\Delta t$

$\sigma_{k+1} - \sigma_k = \Delta\sigma$

new, old indicate iterated values on σ_{k+1}

E_m elasticity of the ice for $\theta = (\theta(t)+\theta(t+\Delta t))/2$

D_k is the self diffusion for $\theta\,(t)$

D_{k+1} - " - for $\theta\,(t + \Delta t)$

For α , K, D and E see chapter 7.

The iteration is started by setting the value $\sigma_{k+1,\,old} := \sigma_k$. Equation (10.12) then gives $\sigma_{k+1,\,new}$. To avoid instability and sometimes to increase the speed of calculations, the new "old" value of the next iteration step is formed by the arithmetic mean of the old and new σ_{k+1}.

$$\sigma_{k+1,\ old} := (\sigma_{k+1,\,new} + \sigma_{k+1,\ old})/2 \qquad \ldots (10.13)$$

The iteration terminates when the difference between the old and new iteration value is less than 10 kN/m^2. If the iteration diverges a printout will be obtained. This has not happened since the operation (10.13) was included.

The iteration is performed for each ice interval and the result is a pressure profile. This profile is integrated over the depth of the ice and gives the total thermal ice pressure per linear meter of the ice cover. The ice pressure is compared to a buckling load (Eq. 7.6) and if this load is exceeded a message is printed.

Maximum Ice Pressure

The calculation above will give a time series of thermal ice pressures. The series will mostly show a daily variation with peak pressures during the afternoons and tension in the early mornings. Because ice has low tensile strength it will crack when tensioned. In the programme the ice pressure is allowed to reach its negative minimum value, but

then the stresses are assumed to be released and they are set to zero in each interval. When the temperature starts to rise again the calculation model will react as if there were no cracks and no old tensile deformations. This will again give an overestimation of occuring pressures.

The maximum positive pressures are obtained by comparing the signs of consecutive increments of the total ice pressure. If the found maximum is greater than 50 kN/m the value is registered along with date, pressure distribution and temperature profile.

In this way a time series of peaks over a threshold is obtained, which series is statistically evaluated in the next paragraph.

11. CALCULATED AND EXPECTED PRESSURES

The time series of maxima over the threshold 50 kN/m has been used to form an annual maximum series and a peaks over a threshold series for each lake. Three types of probability distributions have been fitted to the annual maximum series and tested with a χ^2-test. The series are, however, too short for the used standard method, why the results may be questioned. For the peaks over a threshold series the conditional distribution of magnitudes has been taken to be exponential.

11.1 Annual Maximum Distributions.

In Tables 11.1 - 11.2 the annual maxima for the five lakes are listed. From north to south the maxima over the years are 437, 357, 319, 282 and 256 kN/m. As might have been expected the greatest pressure was thus found in the northernmost lake. The maxima occurred the winters 69/70, 60/61, 70/71, 61/62 and 61/62, the last two at the same time March 8, 1962, 13.00.

The fact that there was no ice on Glan and Vidöstern the winter of 72/73 has caused some trouble, because the true value nil on these yearly maxima gave outliers that were difficult to take into consideration when fitting the statistical distributions.

Table 11.1

ANNUAL MAXIMA FOR TORNE TRÄSK

Winter	Date	Hour	Max Pressure (kN/m)	Remarks
64/65	65 03 07	16	379	
65/66	66 01 29	15	381	
66/67	67 02 19	15	411	
67/68	68 01 28	7	353	
68/69	69 02 23	21	388	
69/70	70 02 22	22	437	highest maximum
70/71	71 03 15	16	271	
71/72	72 03 12	15	402	
72/73	73 03 24	15	343	
73/74	74 02 25	14	283	
74/75	75 04 11	15	376	
75/76	76 04 12	23	302	

Table 11.2

ANNUAL MAXIMA FOR STORA BYGDETRÄSKET

60/61	61 03 23	13	357	highest maximum
61/62	61 12 28	13	131	
62/63	63 01 19	15	286	
63/64	64 01 29	14	330	
64/65	65 01 12	6	250	
65/66	66 01 01	13	283	
66/67	67 04 19	16	202	
67/67	67 12 28	23	156	
68/69	68 12 21	13	239	
69/70	70 05 09	8	130	
70/71	71 01 08	0	281	
71/72	72 01 31	20	267	
72/73	73 01 10	3	212	
73/74	74 04 11	10	209	
74/75	75 03 22	16	252	
75/76	75 12 21	13	222	

Table 11.3

ANNUAL MAXIMA FOR RUNN

Winter	Date	Hour	Max Pressure (kN/m)	Remarks
60/61	61 02 24	14	236	
61/62	61 12 28	0	267	
62/63	63 04 25	12	212	
63/64	64 03 14	14	274	
64/65	65 03 26	15	251	
65/66	66 04 18	18	193	
66/67	67 03 24	13	209	
67/68	68 03 17	17	255	
68/69	69 03 13	14	283	
69/70	70 01 10	20	114	
70/71	71 01 07	18	318	highest maximum
71/72	72 03 30	16	208	
72/73	73 03 25	12	147	
73/74	74 04 12	14	267	
74/75	75 03 23	14	257	
75/76	76 01 08	12	236	

Table 11.4

ANNUAL MAXIMA FOR GLAN

60/61	61 01 28	13	161	
61/62	62 03 08	13	282	highest maximum
62/63	63 03 14	14	274	
63/64	64 03 28	14	237	
64/65	65 03 26	14	238	
65/66	66 04 13	13	233	
66/67	67 02 12	13	194	
67/68	68 03 14	15	221	
68/69	69 02 14	13	226	
69/70	69 12 11	21	71	
70/71	71 01 31	13	177	
71/72	72 03 20	12	184	
72/73			----	no ice cover
73/74	73 12 10	7	196	
74/75	75 03 31	9	150	
75/76	76 03 13	17	159	

Table 11.5

ANNUAL MAXIMA FOR VIDÖSTERN

Winter	Date	Hour	Max Pressure (kN/m)	Remarks
60/61	61 01 26	15	189	
61/62	62 03 08	13	256	highest maximum
62/63	63 04 03	15	152	
63/64	64 02 20	15	236	
64/65	65 03 10	21	159	
65/66	66 02 14	16	193	
66/67	67 03 17	11	166	
67/68	68 02 17	16	244	
68/69	69 02 15	13	230	
69/70	70 02 06	21	112	
70/71	71 03 12	17	187	
71/72	72 03 26	14	164	
72/73			---	no ice cover
73/74	73 12 19	22	121	
74/75	75 02 16	14	145	
75/76	76 03 18	14	243	

Fitted Distributions

The arithmetic mean $\bar{x}$, standard deviation s, coefficient of variation $C_V = s/\bar{x}$ and skewness g, are listed in Table 11.6 below for the samples of annual maxima. For the lakes Glan and Vidöstern two populations have been formed called I and II, in the latter of which the "annual maxima" 0 kN/m have been skipped. As will be shown below the samples Glan II and Vidöstern II fit selected distributions better.

Table 11.6
Arithmetic mean $\bar{x}$, standard deviation s, coefficient of variation C_v, and skewness g for the samples of annual pressure maxima. N is the size of the samples.

	N	$\bar{x}$ (kN/m)	s (kN/m)	C_v	g	$3C_v+C_v^3$
Torne träsk	12	360.50	51.95	0.144	-0.545	0.435
Stora Bygdeträsket	16	237.94	64.75	0.272	-0.096	0.837
Runn	16	232.94	51.59	0.221	-0.832	0.675
Glan I	16	187.69	72.10	0.384	-1.2973	----
II	15	200.20	53.72	0.268	-0.6996	0.823
Vidöstern I	16	174.81	64.68	0.370	-1.1823	----
II	15	186.47	46.41	0.249	0.0538	0.762

Three two-parameter distributions have been fitted to the samples, namely the normal, the lognormal and the Gumbel distribution. The parameters of these distributions are evaluated by means of the method of moments. See for example Flood Studies Report (1975). The result is as follows:

Normal distribution

$$f(x) = \frac{1}{\sigma\sqrt{2\pi}} \exp - \left[\frac{x-\mu}{\sigma\sqrt{2}}\right]^2 \qquad \ldots (11.1)$$

$$\text{Mean } \mu = \bar{x} = \frac{1}{N}\sum_{i=1}^{N} x_i$$

$$\text{Variance } \sigma^2 = s^2 = \left[\frac{1}{N-1}\sum_{i=1}^{N}(x_i - \bar{x})^2\right]^{1/2}$$

$$\text{Skewness } g = 0$$

Lognormal distribution

$$f(x) = \frac{1}{\sigma_n\sqrt{2\pi}} \exp - \left[\frac{\ln x - \mu_n}{\sqrt{2}\,\sigma_n}\right]^2 \qquad \ldots (11.2)$$

$$\text{Mean } \mu_n = \bar{x}_n = \frac{1}{N} \sum_{i=1}^{N} \ln x_i$$

$$\text{Variance } \sigma_n^2 = s_n^2 = \left[\frac{1}{N-1} \sum_{i=1}^{N} (\ln x_i - \bar{x}_n)^2 \right] 1/2$$

Skewness of $\ln x$ $g_n = 0$

If the sample x fits the lognormal distribution the skewness of $\ln x$ is $g_n = 0$ but the skewness of the original sample x is $g = 3\, C_v + C_v^3$ where C_v is estimated as $s/\bar{x}$.

Gumbel or Extreme Value Type I distribution

$$f(x) = \alpha \exp \left[-\alpha (x - \beta) - \exp (-\alpha (x - \beta)) \right] \qquad \ldots (11.3)$$

$\alpha = 1.28/\sigma = k_1/s$
$\beta = \mu - 0.450\sigma = \bar{x} - k_2 \cdot s$

$\bar{x}$ and s are the sample mean and standard deviation as for the normal distribution. For big samples ($N > 200$) k_1 approaches 1.28 and k_2 0.45. For small samples the coefficients are chosen according to Gumbel (1958). The skewness is constant with $g = 1.14$.

All three two-parameter distributions have been estimated by the sample mean and standard deviation. The values of skewness for the samples of annual maxima are negative with the exception of the sample from Vidöstern II which is slightly positively skewed. Of the fitted distributions the normal distributions with $g = 0$ are closest to the skewness of the samples. Maybe a three-parameter distribution with negative skewness would have given a better fit to the values. A possible distribution is the Pearson Type III distribution. The samples are, however, so short that it is difficult to draw far-reaching conclusions.

The parameters of the fitted distributions are listed below in Table 11.7, 11.8 and 11.9, and the annual maxima are plotted in Figures 11.1-5. The plotting position is given by the Weibull formula $p_i = i/(N+1)$ where i is the ranking number. The curves of the fitted distributions are also drawn in the figures.

Table 11.7

PARAMETERS OF THE FITTED NORMAL DISTRIBUTIONS

Lake	$\bar{x}$ (kN/m)	s (kN/m)
Torne träsk	360.50	51.95
Stora Bygdeträsket	237.94	64.75
Runn	232.94	51.59
Glan I	187.69	72.10
Glan II	200.20	53.72
Vidöstern I	174.81	64.68
Vidöstern II	186.47	46.41

Table 11.8

PARAMETERS OF THE FITTED LOGNORMAL DISTRIBUTIONS.
$\bar{x}_n = \overline{\ln x}$ with x in kN/m.

Lake	$\bar{x}_n$	s_n
Torne träsk	5.8772	0.1513
Stora Bygdeträsket	5.4333	0.2966
Runn	5.4228	0.2583
Glan II	5.2550	0.3354
Vidöstern II	5.1979	0.2587

Table 11.9
PARAMETERS OF THE FITTED GUMBEL DISTRIBUTIONS

Lake	α (m/kN)	β (kN/m)
Torne träsk	0.018865	333.78
Stora Bygdeträsket	0.015907	205.75
Runn	0.019966	207.29
Glan I	0.014286	151.85
Glan II	0.018988	173.34
Vidöstern I	0.015925	142.66
Vidöstern II	0.021978	163.26

From the plotted distributions one may visually draw the conclusion that the Gumbel distribution does not fit the samples as closely as the other two distributions. The greatest pressures seem to be very over-estimated. A choice between the normal and lognormal distributions is more difficult to make just by the shape of the curves. For Glan and Vidöstern it can be observed that the samples that include the annual maxima zero hardly can be fitted by any of the tested distributions. The extreme pressures would be unreasonably over-estimated. See Table 11.12 below.

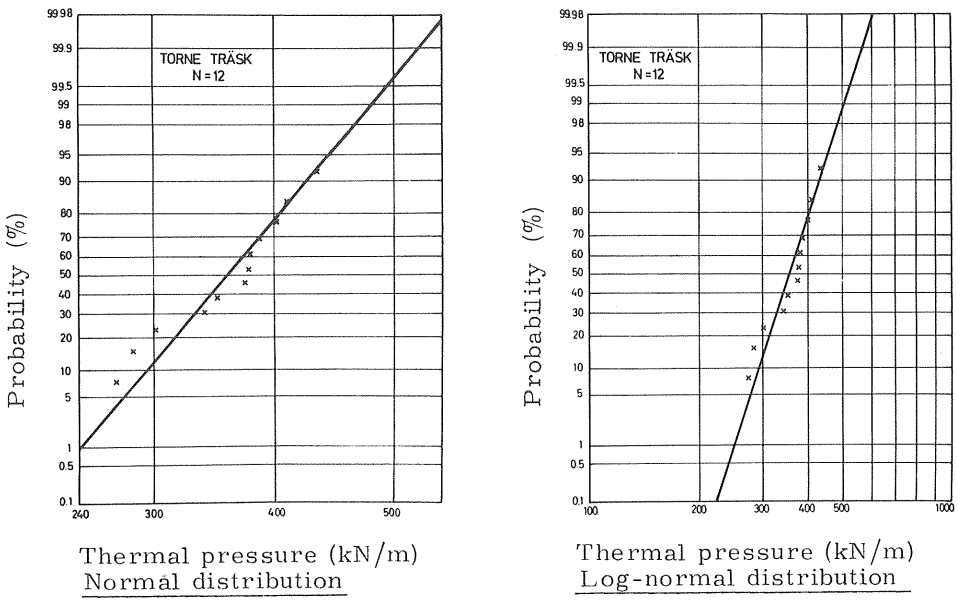

Figure 11.1 Plotted sample and fitted distributions for Torne träsk. Annual-maximum series.

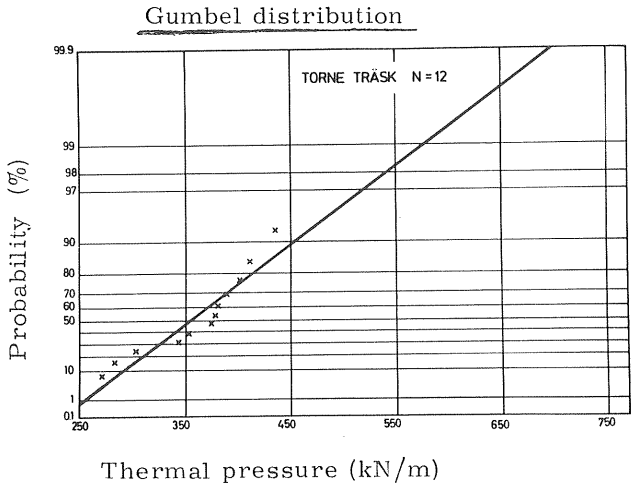

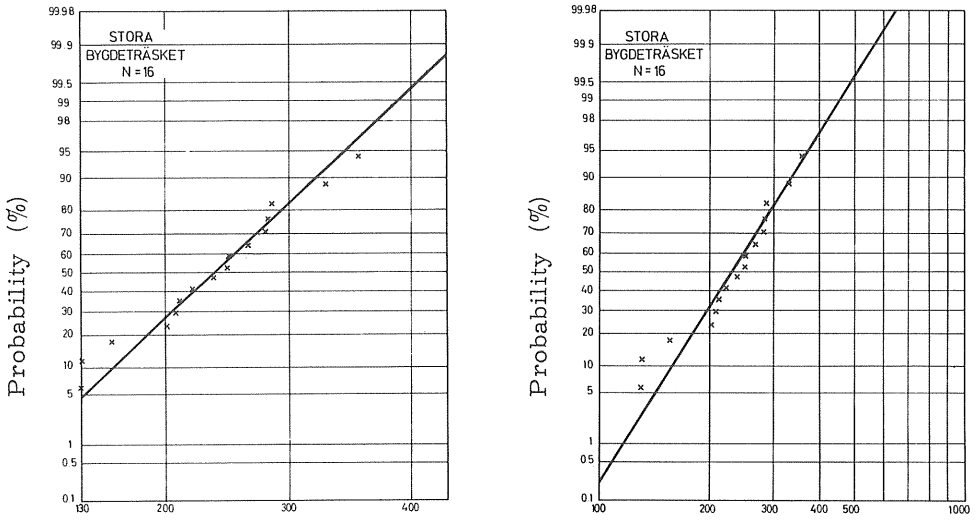

Figure 11.2 Plotted sample and fitted distributions for Stora Bygdeträsket. Annual-maximum series.

Gumbel distribution

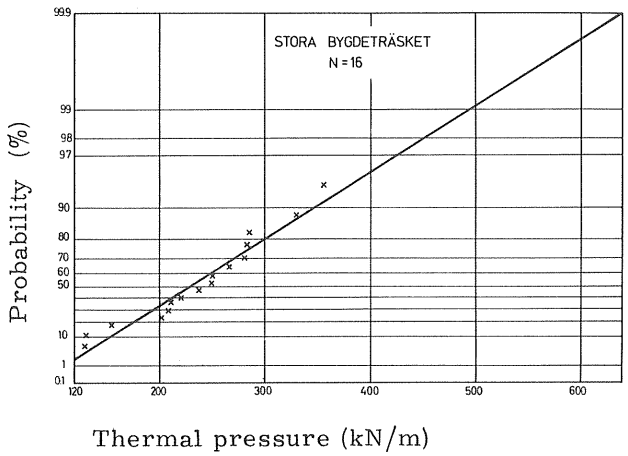

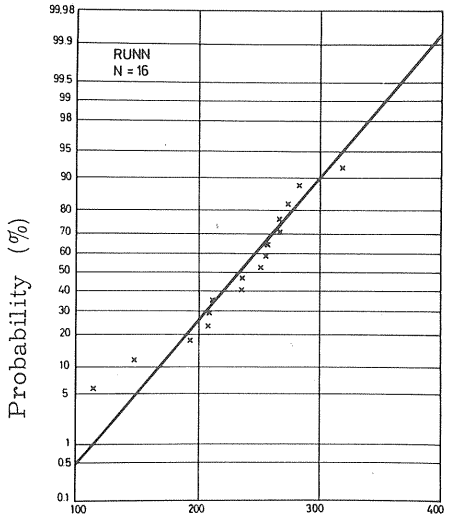

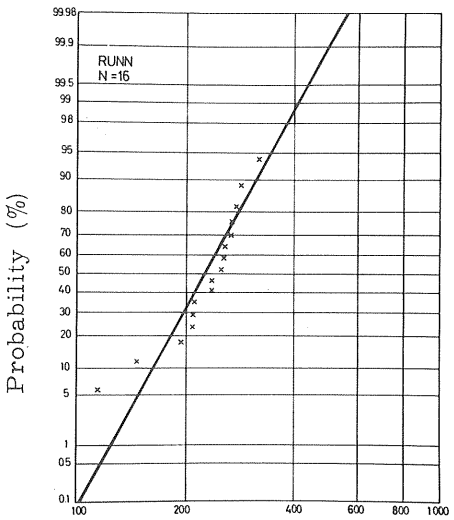

Figure 11.3 Plotted sample and fitted distributions for Runn. Annual-maximum series.

Gumbel distribution

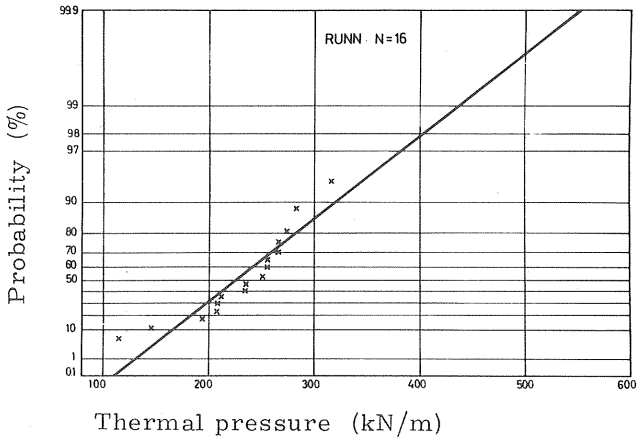

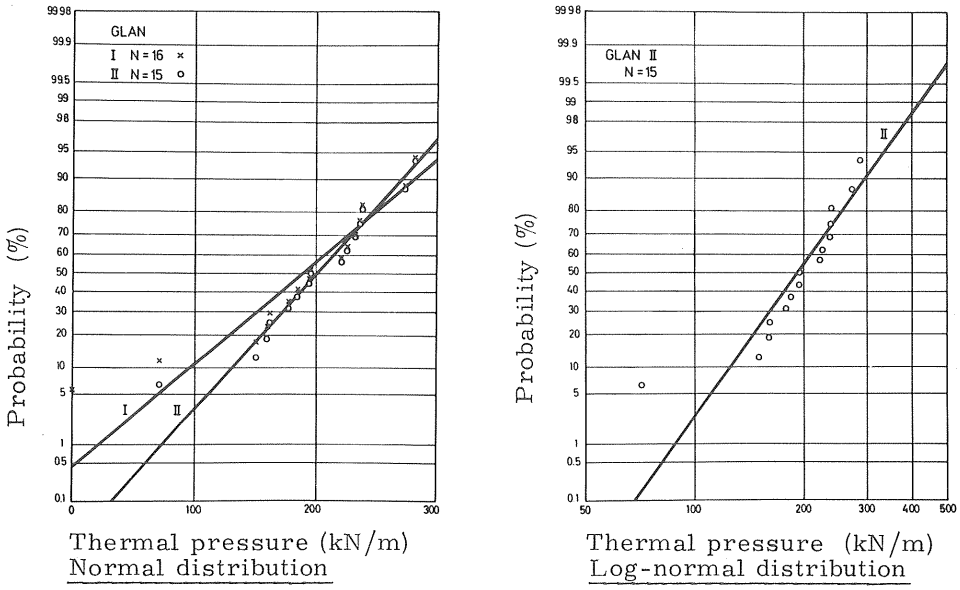

Figure 11.4 Plotted samples and fitted distributions for Glan. Annual maximum series.

Gumbel distribution

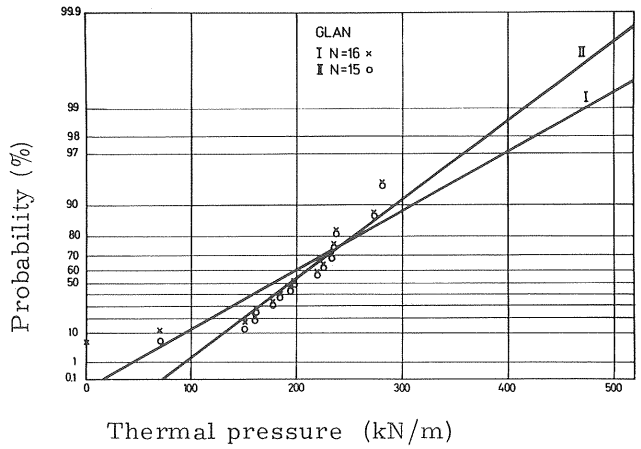

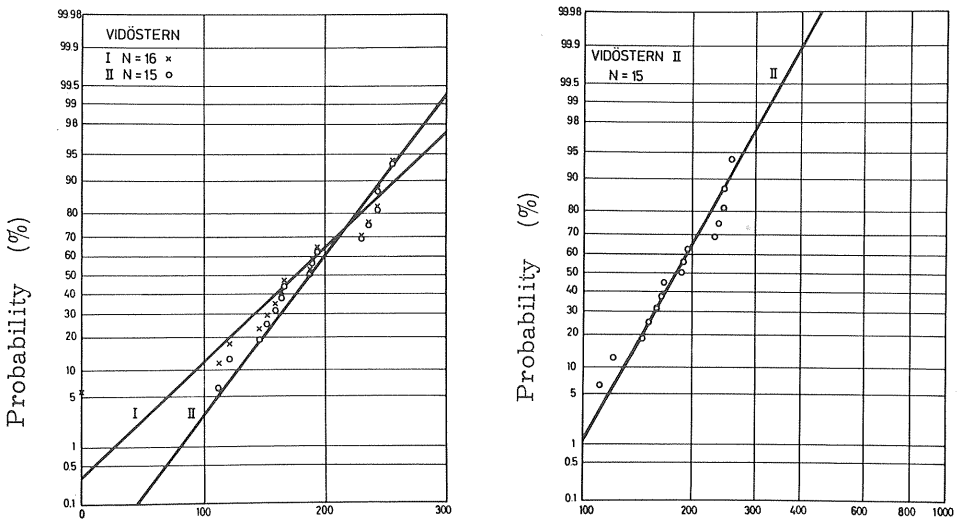

Figure 11.5 Plotted samples and fitted distributions for Vidöstern. Annual-maximum series.

Gumbel distribution

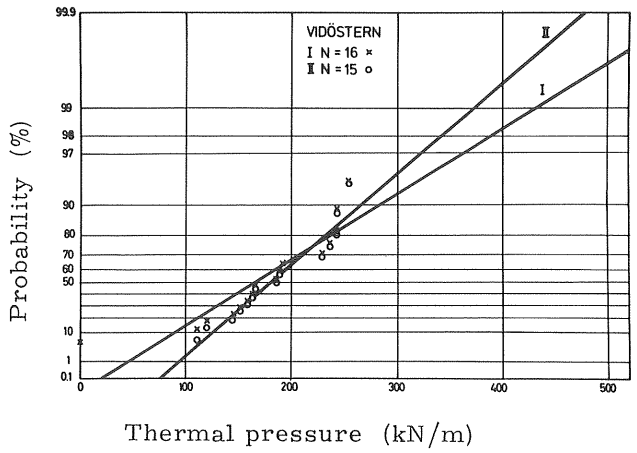

Chi square test

The quality of the fitted distributions has been tested by a chi-square test although this should not be done when a sample is smaller than 20. The χ^2-quantity is tabulated in Table 11.10. Five classes were used and the distribution was estimated by two parameters. Thus the test quantity is χ^2-distributed with two degrees of freedom. If the mean of the test quantity is taken for the three types of distributions the ranking order of the distributions is normal, lognormal and Gumbel distribution. It is interesting to note that χ^2 for the normal distributions of Glan I and Vidöstern I are small although the distributions fit extreme values very poorly.

Table 11.10 χ^2 and $P(\chi^2)$ for fitted annual-maximum distributions. Two degrees of freedom.

	Normal		Lognormal		Gumbel	
	χ^2	$P(\chi^2)$	χ^2	$P(\chi^2)$	χ^2	$P(\chi^2)$
Torne Träsk	2.33	<0.75	5.00	<0.95	8.67	<0.99
Stora Bygdeträsket	0.75	<0.50	1.75	<0.75	2.50	<0.75
Runn	3.75	<0.90	3.75	<0.90	3.75	<0.90
Glan I	0.50	<0.25	-	-	7.50	<0.99
Glan II	1.00	<0.50	2.33	<0.75	2.33	<0.75
Vidöstern I	2.00	<0.75	-	-	6.75	<0.975
Vidöstern II	2.07	<0.75	0.20	<0.10	0.47	<0.25

For the significant levels, 1 - P (χ^2), 0.10, 0.05, and 0.01 the number of times out of five (Glan I and Vidöstern I excluded) that each type of distribution is rejected is listed in Table 11.11 below. The differences are inconclusive, which can be interpreted as a consequence of the small samples. Great deviations from the parent distributions are expected for realizations of any statistical variable if the sample is as small as in these cases. A conservative interpretation of the test would be that only the normal distributions should be accepted, because on the significant level 10 % the average percentage of realizations with $P(\chi^2) \geq 0.90$ should be 10 %, while in this case the percentages are 0,20 and 20 % respectively for the distributions.

Table 11.11

Number of times out of five that each type of distribution is rejected by chi-square test.

Significant level	Normal	Lognormal	Gumbel
0.10	0	1	1
0.05	0	0	1
0.01	0	0	0

Expected Pressures

Expected pressures calculated from the fitted distributions of annual maxima for the periods of recurrence 100, 500 and 1000 years are given in Table 11.12. For the reasons just accounted for the normal or lognormal distributions are preferred. Conservative values are given by the latter, and the pressures for the recurrence 100 years are from north to south 507, 453, 410, 419 and 330 kN/m.

Table 11.12

Expected thermal ice pressures for the recurrence period 100, 500, and 1000 years according to the three tested types of distributions.

Period of recurrence (years)		100			500			1000		
Sample size N, type of distribution	N	N	L	G	N	L	G	N	L	G
Torne träsk	12	480	507	577	509	550	661	520	569	698
Stora Bygdeträsket	16	388	453	494	424	532	596	438	568	640
Runn	16	353	410	436	381	475	517	392	500	550
Glan I	16	355	-	474	394	-	587	410	-	663
Glan II	15	324	419	415	353	507	500	365	543	536
Vidöstern I	16	325	-	432	360	-	534	374	-	577
Vidöstern II	15	294	330	372	320	380	446	330	400	478

N = Normal Distribution
L = Lognormal -"-
G = Gumbel -"-

11.2 Peaks over a Threshold Series

In order to increase the size of the samples a peaks over a threshold series have been tested with an exponential function for the distribution of magnitudes. The average number of peaks per year was taken to three so that the size of the sample became 3N, where N is the number of years. In this way samples were formed that were allowed to be tested by a chi-square test as the number of peaks became enough. Furthermore, the problem that there were no pressures in Glan and Vidöstern one winter disappeared automatically. A new problem may be that the peaks must not be too close to one another, in which case they might not be statistically independent. Below this last aspect is disregarded. From the listed values it can be seen that the ranked pressures often comes from days very close to each other. In a few cases they even belong to the same day.

In Tables 11.13 to 11.17 below the peaks over a threshold series are listed for the five lakes. The highest maxima in these series are of course the same as in the earlier annual-maximum series. The series are plotted in Figures 11.6 - 11.10.

Table 11.13

PEAKS OVER A THRESHOLD SERIES FOR TORNE TRÄSK

Date	Hour	Pressure (kN/m)
70 02 22	22	437
67 02 27	16	411
67 02 21	3	406
67 02 21	13	403
72 03 12	15	402
69 02 23	21	388
66 01 29	15	381
65 03 07	16	379
67 02 19	15	379
75 04 11	15	376
72 03 13	14	375
65 03 08	14	375
69 02 24	22	367
70 02 22	2	363
65 03 08	2	362
65 03 12	15	357
66 01 06	8	356
65 03 06	16	353
68 01 28	7	353
69 05 02	16	353
72 04 07	15	349
69 05 01	16	349
67 03 06	16	348
69 02 25	14	343
66 03 14	21	343
72 02 19	13	343
73 03 24	15	343
66 03 13	18	342
67 02 22	16	340
66 03 17	18	338
68 01 21	7	337
70 01 21	13	337
67 01 16	13	334
66 01 22	18	334
72 02 19	1	333
68 01 13	18	331

Table 11.14

PEAKS OVER A THRESHOLD SERIES FOR STORA BYGDETRÄSKET

Date	Hour	Pressure (kN/m)
61 03 23	13	357
64 01 29	14	330
64 02 03	22	314
61 03 21	15	293
63 01 19	15	286
66 01 01	13	283
71 01 08	0	281
71 01 20	14	278
63 01 18	15	273
72 01 31	20	267
64 01 29	5	263
72 02 01	15	258
64 01 18	13	257
61 03 15	14	256
63 01 22	19	255
75 03 22	16	252
75 03 19	14	252
61 03 20	15	250
65 01 12	6	250
75 03 19	1	250
71 12 13	22	250
61 03 09	17	246
61 03 19	15	246
63 01 11	16	242
63 01 13	16	241
71 01 09	2	240
68 12 21	13	239
71 01 01	20	233
75 03 21	16	230
75 03 25	15	227
75 03 02	21	225
64 01 17	14	225
63 01 12	15	224
75 03 04	15	224
75 03 03	14	223
75 12 21	13	222
66 01 01	8	221
63 01 22	3	219
61 03 17	16	219
63 01 23	22	217
71 01 19	14	216
65 01 13	20	216
75 12 20	13	216
72 03 29	15	213
64 01 30	14	213
75 03 26	15	212
75 03 23	16	212
73 01 10	3	212

Table 11.15

PEAKS OVER A THRESHOLD SERIES FOR RUNN

Date	Hour	Pressure (kN/m)
71 01 07	18	318
71 01 08	10	297
69 03 13	14	283
64 03 14	14	274
69 03 14	15	270
61 12 28	0	267
74 04 12	14	267
69 03 09	14	261
64 03 16	15	259
75 03 23	14	257
68 03 17	17	255
71 02 04	14	255
71 02 03	14	253
64 03 20	15	253
65 03 26	15	251
64 03 28	16	251
75 03 14	15	250
64 03 22	15	249
75 03 19	15	248
69 03 10	15	247
62 01 16	20	247
75 03 18	15	246
64 03 26	16	245
69 03 11	15	244
75 03 22	14	243
61 12 28	10	241
69 03 12	15	241
64 03 15	15	240
64 03 25	16	240
74 01 24	19	240
75 03 13	15	239
61 02 24	14	236
76 01 08	12	236
74 02 21	14	234
61 02 23	14	233
75 03 21	15	232
65 03 23	16	231
74 03 23	15	231
64 03 21	15	229
75 04 17	13	228
75 03 12	15	228
64 01 21	12	226
64 03 27	16	226
65 03 25	14	226
76 03 08	15	226
68 04 09	15	226
61 02 22	14	225
64 01 29	13	225

Table 11.16

PEAKS OVER A THRESHOLD SERIES FOR GLAN

Date	Hour	Pressure (kN/m)
62 03 08	13	282
63 03 14	14	274
63 03 15	14	267
63 03 22	14	262
63 03 21	14	258
63 03 16	14	256
65 03 26	14	238
64 03 28	14	238
63 03 23	14	235
63 03 17	14	233
66 04 13	13	233
62 03 06	15	228
63 03 28	14	228
63 04 01	14	227
69 02 14	13	226
66 01 02	1	222
68 03 14	15	221
64 04 05	14	219
65 03 27	15	215
64 03 17	14	214
64 04 03	14	214
62 02 28	15	211
62 02 16	12	211
65 03 22	14	209
63 03 31	14	209
64 03 27	15	203
65 03 23	14	203
64 04 02	14	203
62 03 07	17	202
69 02 15	13	199
64 03 18	14	198
64 03 26	15	196
68 03 18	13	196
73 12 10	7	196
63 04 02	15	195
67 02 12	13	194
64 03 21	15	192
66 04 12	14	191
66 04 16	13	189
66 04 15	14	187
63 03 20	14	187
63 03 24	16	186
64 04 09	13	185
64 03 22	14	184
72 03 20	12	184
63 03 27	14	183
64 04 04	15	180
68 03 21	13	178

Table 11.17

PEAKS OVER A THRESHOLD SERIES FOR VIDÖSTERN

Date	Hour	Pressure (kN/m)
62 03 08	13	256
68 02 17	16	244
76 03 18	14	244
64 02 20	15	236
64 02 21	13	233
69 02 15	13	230
76 03 19	14	228
62 03 06	15	228
64 03 28	14	223
64 04 02	14	223
62 03 07	15	222
62 02 23	14	219
76 03 12	14	218
62 03 01	15	216
64 03 27	15	215
62 03 05	15	215
64 02 19	15	208
62 03 09	15	208
64 04 03	15	208
76 01 31	15	207
76 02 16	14	206
64 03 26	15	206
76 03 14	15	205
68 02 16	15	204
69 04 03	11	203
76 02 07	14	201
76 01 31	19	199
76 03 20	15	199
62 02 16	8	199
76 03 13	15	193
66 02 14	16	193
61 01 26	15	189
69 02 14	13	188
71 03 12	17	187
68 02 14	14	187
76 02 06	14	184
76 03 17	15	182
68 02 15	13	181
66 02 21	16	180
76 01 18	14	179
69 04 09	10	179
76 03 16	14	178
76 01 30	14	176
64 04 08	10	176
64 02 13	16	174
76 02 28	14	174
76 02 21	15	173
69 04 05	11	172

Fitted Exponential Distributions

An exponential distribution has been fitted to the threshold series according to a method described in Flood Studies Report (1975). The pressure P(T) with the recurrence T years is given by

$$P(T) = x_o + \beta (\ln \lambda + \ln T) \quad \ldots (11.4)$$

where x_o is the probable threshold for a fixed number of exceedances per year, which is estimated as

$$x_o = x_{min} - \frac{\beta}{\lambda N} \quad \ldots (11.5)$$

$$\beta = \frac{\lambda N}{\lambda N - 1} (\bar{x} - x_{min}) \quad \ldots (11.6)$$

x_{min} is the smallest value of the series

β a parameter

λ number of exceedances in average per year

N number of years

$\bar{x}$ arithmetic mean over λN values

The parameters β and x_o are given in Table 11.18 below, and the lines for the fitted distributions are drawn in figures 11.6-11.10. It can be seen that the lines fit the plotted values very well for the three northern lakes, while the fitness is rather poor for the southernmost lake Vidöstern.

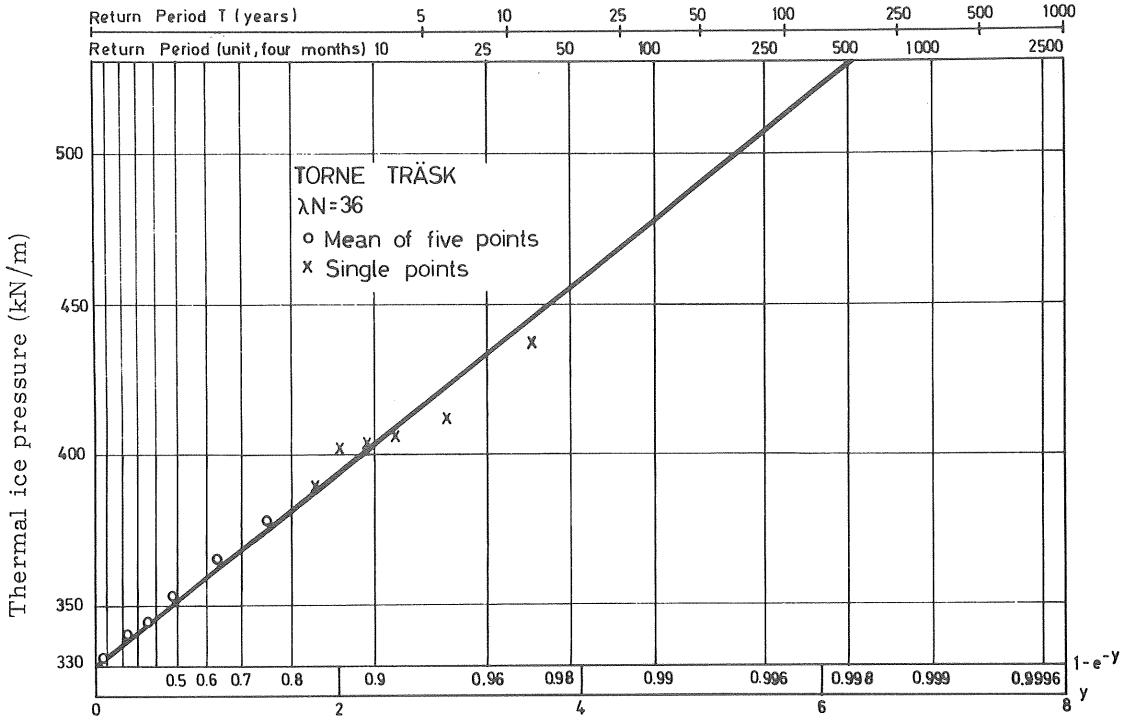

Fig. 11.6 Plotted sample and fitted distribution for Torne träsk. Exponential threshold distribution.

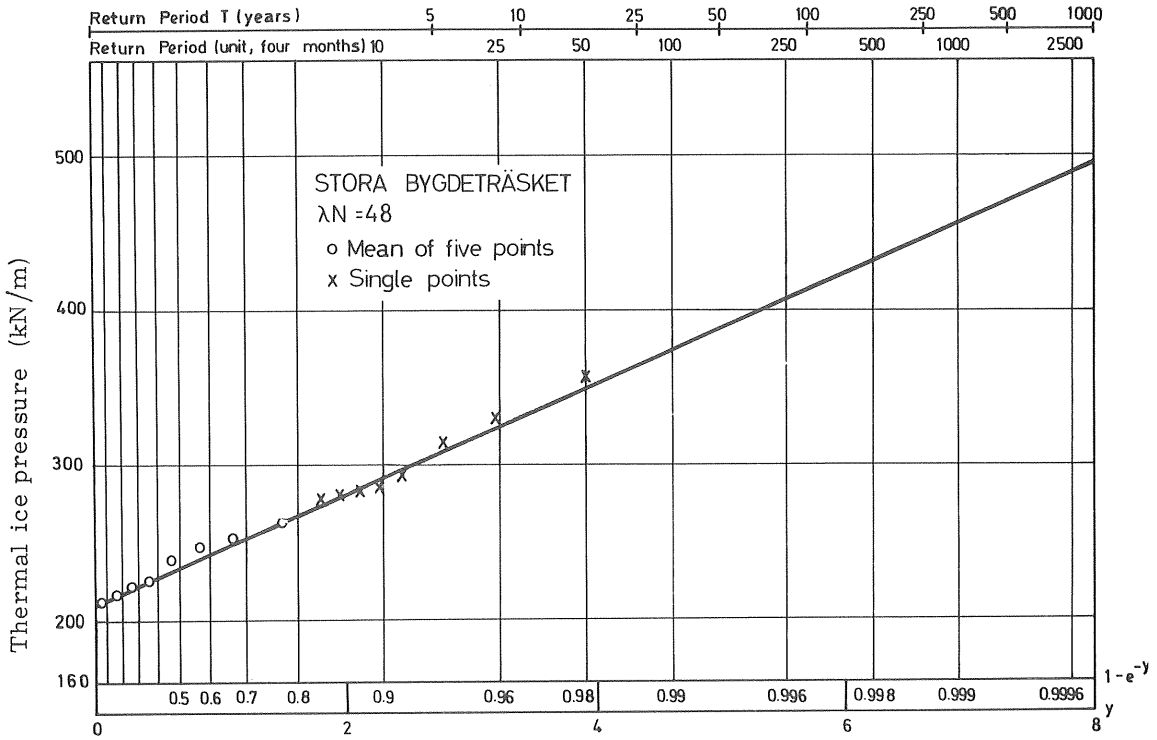

Fig. 11.7 Plotted sample and fitted distribution for Stora Bygdeträsket. Exponential threshold distribution.

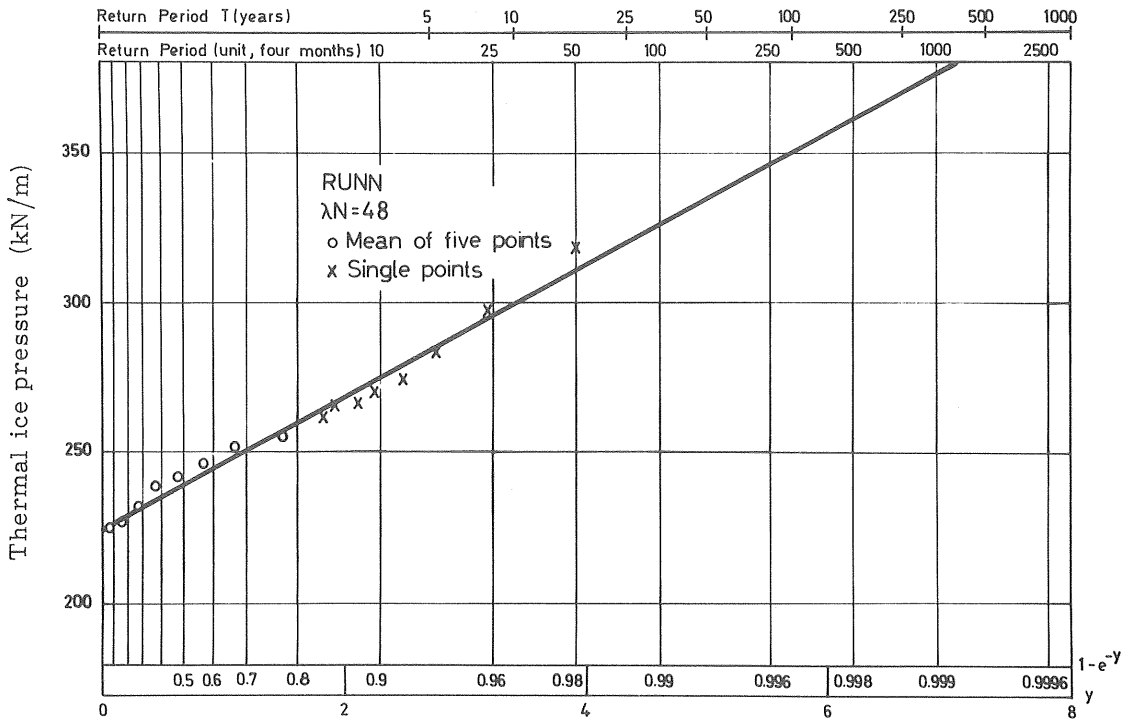

Fig. 11.8 Plotted sample and fitted distribution for Runn.
Exponential threshold distribution.

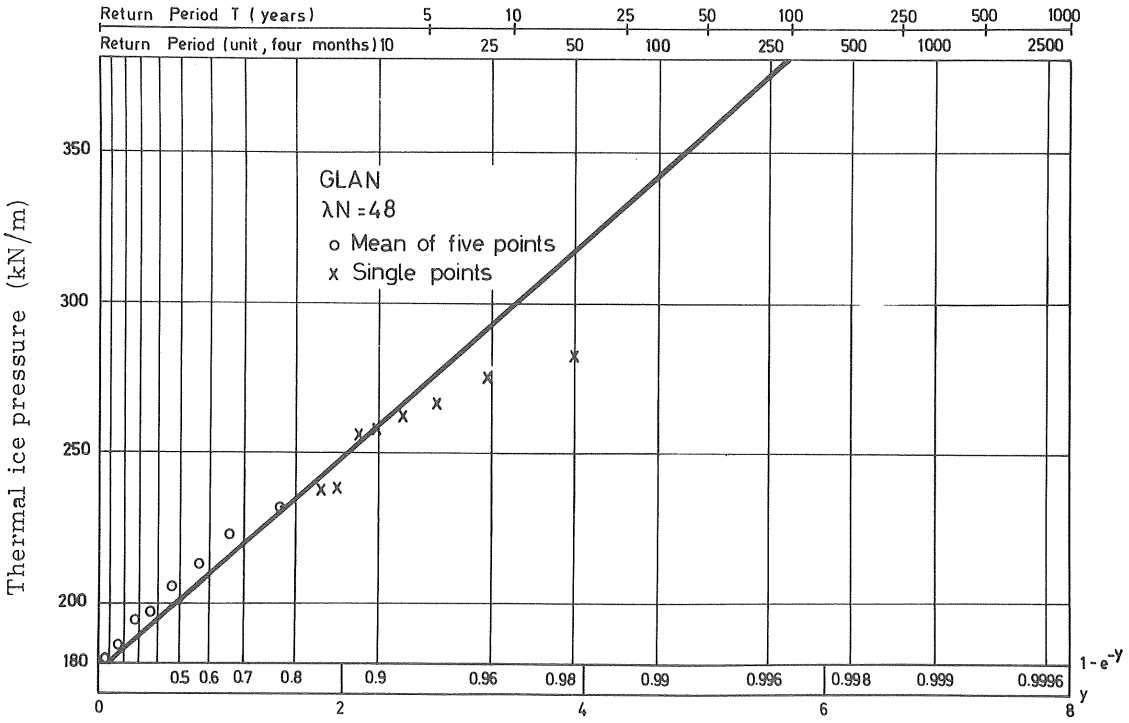

Fig. 11.9 Plotted sample and fitted distribution for Glan.
Exponential threshold distribution.

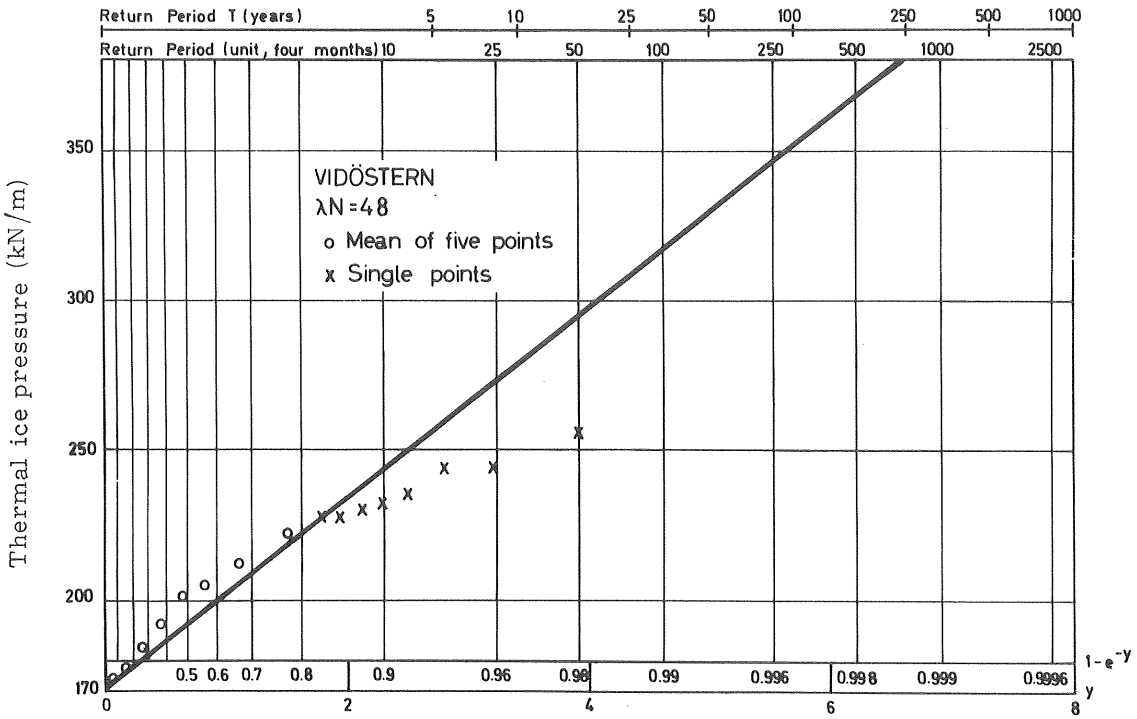

Fig. 11.10 Plotted sample and fitted distribution for Vidöstern. Exponential threshold distribution.

Table 11.18

The parameters β and x_o of the fitted peaks over a threshold series.

	λN	β (kN/m)	x_o (kN/m)
Torne träsk	36	31.57	330.2
Stora Bygdeträsket	48	35.53	210.9
Runn	48	21.94	224.6
Glan	48	35.69	177.7
Vidöstern	48	31.59	171.5

Chi-Square Test

The fitted exponential distributions have been tested with a chi-square test, the result of which is listed in Table 11.19. It is seen that only the Vidöstern distribution is rejected on the significant level 10 %, and none is rejected on the level 5 and 1 %. Thus, the average number of rejections is 20 % (one out of five) for the level 10 % while it should be approximately equal to that percentage. As before a conservative conclusion would be to reject the fitted type of distribtuion on the level 10 %. The number of samples is, however, too small for such conclusions.

Table 11.19

χ^2 and $P(\chi^2)$ for the peaks over a threshold series.
r = degrees of freedom.

	λN	r	χ^2	$P(\chi^2)$
Torne träsk	36	4	3.3	<0.50
Stora Bygdeträsket	48	6	5.8	<0.75
Runn	48	6	6.7	<0.75
Glan	48	6	4.3	<0.50
Vidöstern	48	6	10.8	<0.95

Expected Pressures

The expected pressures with the periods of recurrence 100, 500 and 1000 years for the fitted exponential distributions are listed in Table 11.20.

Table 11.20 Expected thermal ice pressure for the recurrence period 100, 500 and 1000-years according to the exponential distribution for the peaks over a threshold.

	Sample size	Period of Recurrence (years)		
	λN	100	500	1000
Torne träsk	36	510	561	583
Stora Bygdeträsket	48	414	471	495
Runn	48	350	385	400
Glan	48	381	440	463
Vidöstern	48	352	402	424

11.3 The Annual-Maximum Series versus the Peaks over a Threshold Series

When comparing the expected pressures according to the annual-maximum series Table 11.12 and the expected pressures according to the peaks over a threshold series Table 11.20, it is seen that the pressures agree roughly for the log-normal distribution of annual maxima and the exponential distribution of peaks over a threshold. For Stora Bygdeträsket the pressures for the threshold series are smaller and intermediate to the normal and lognormal distributions. For Runn they are still smaller and closer to the normal distribution.

In spite of the fact that the problem of statistical independence was disregarded, the threshold series did not give statistical extrapolations of extreme pressures much different from the annual-maximum series. In fact the independence condition is grossly violated. For example, for Torne träsk the pressures ranked as number 3 and 4 were calculated for the same day 67-02-21 at 3.00 and 13.00. In the same series number 8, 12, 15, 16 and 18 would have occurred during March 6-12, 1965.

It can be noted that for very rare events the exponential and Gumbel distribution should converge for the same sample.

12. RESULT

Provided the mathematical model used for the calculation of the thermal ice pressure is accepted, the study has produced statistical estimates of the magnitude of the thermal ice pressure that can be expected in the ice covers on the five lakes. The most reliable figures on expected pressures are given by the fitted log-normal distributions for the five studied lakes. One must notice, however, that the computed time series are very short. In Table 11.21 below the estimates of the thermal ice pressure with the recurrence 100, 500 and 1000 years are repeated for the log-normal distribution. Its parameters are given in Table 11.8. Values from the other fitted distributions are given in tables 11.12 and 11.20.

Table 11.21 Expected thermal ice pressures for the recurrence period 100, 500, and 1000 years according to the fitted log-normal distributions of annual maxima.

	Sample size	Period of Recurrence 100	500	1000
Torne träsk	12	507	550	569
Stora Bygdeträsket	16	453	532	568
Runn	16	410	475	500
Glan	15	419	507	543
Vidöstern	15	330	380	400

13. RECOMMENDATIONS

As has been pointed out the lengths of the computed pressure series were limited by the fact that the weather observations were not filed on magnetic tape. A primary improvement of this work would be to complete the series between 1940 and 1978. If no alterations are made in the ice-pressure programme the main effort of this task would be to convert the weather observations into computer accessible form. If observations are lacking for any period these should be faked by a stochastic model or by taking data from a neighbouring meteorological station.

Once the time series have been completed, one has a better opportunity to test suitable statistical distributions as the number of annual maxima would increase from 12 and 16 to 37 for the lakes. The testing should include other types of distributions as well as an investigation of the criteria of statistical independence of the peaks over a threshold series.

If the rheological model used in the computations is not accepted it can with a moderate effort be exchange for another type, or its constants can be changed. The direct computational costs are relatively small.

A wider development would be to build a numerical model for sea areas, which might be of interest for the future building of bridges between Åland and Sweden or Finland. Such a work involves a complete renewal of the thermal part of the computer programme as well as changes in the rheological part. The effort becomes great.mainly because of the nature of columnar sea ice with its phase changes and inclusions of brine.

LIST OF TABLES

LIST OF FIGURES

LIST OF NOTATIONS

A	coefficient of heat transfer	$W/(m^2 \cdot K)$
A	absolute fusion temperature of water	K
A	tridiagonal matrix	
a	temperature diffusivity	m^2/s
a	constants	
B	Bowen´s ratio	-
B	tridiagonal matrix	
b	constants	
C	cloud cover in eighths (octas)	-
C_p	specific heat capacity	$J/(kg \cdot K)$
C_v	coefficient of variation	-
c	constants	
D	self diffusion of the molecules in ice	m^2/s
D	number of the day in a year with D = 1 for January 1	
D	column vector of terms that do not depend on ice temperatures	
D_o	constant	m^2/s
d	differential operator	-
E	modulus of elasticity	Pa
E_r	elasticity of ice for time averaged temperature	Pa
e	saturation vapour pressure at the ice surface	Pa
e_a	water vapour pressure of the air	Pa
f(u)	wind-speed function	m/s
f(x)	probability density function	-
GMT	Greenwich time	h
g	earth acceleration	m/s^2
g	skewness for f(x) or sample	-
g_n	skewness for ln x	-
H	solar time of the day	h
h	thickness of ice cover	m
h	local hour angle of the sun	rad
i	order number of interval limit	-
J	short-wave radiation flux	W/m^2

K	coefficient for viscous deformation	m^{-2}
k	absorption coefficient	m^{-1}
k	number of point of time $t = k\Delta t$	-
k	constant	
k_1, k_2	parameters of Gumbel distribution	-
L	specific heat of fusion	J/kg
L_s	specific heat of sublimation	
N	sample size	-
N	number of years	-
n	exponent for viscous deformation	-
new	latest iterated value of σ_{k+1}	-
O	ordo, of the order of	-
old	second latest iterated value of σ_{k+1}	-
P(T)	ice pressure with the recurrence interval T	N/m
P(t)	thermal ice pressure as a function of time	N/m
P_b	buckling load	N/m
p	effect source per unit volume	W/m^3
Q_s	activation energy for self diffusion	J/mol
q	heat flux	W/m^2
q	time average of source term p containing terms dependent on surface temperature	W/m^3
q_b	emitted long-wave radiation flux	W/m^2
q_c	solar and sky radiation flux reduced by cloud cover	W/m^2
q_{CL}	short-wave irradiation through a horizontal surface	W/m^2
q_c	total convective heat transfer	W/m^2
q_e	latent heat transfer	W/m^2
q_l	absorbed long-wave radiation flux	W/m^2
q_{la}	long-wave radiation emitted by the atmosphere	W/m^2
q_{lc}	long-wave radiation emitted by the atmosphere by cloudy weather	W/m^2
q_S	sensible heat transfer	W/m^2
q_s	absorbed short-wave radiation flux	W/m^2
R	the universal gas constant	$J/(mol \cdot K)$
r	reflection coefficient	-
s	sample standard deviation	kN/m

s_n	sample standard deviation of ln x	-
T	absolute temperature	K
T	recurrence interval	years
T_a	absolute temperature of the air	K
T_1	column vector of old (known) temperatures	^oC
T_2	column vector of new (unknown) temperatures	^oC
t	point of time	s
u	wind speed	m/s
x	vertical coordinate	m
x	statistical variable	kN/m
$\bar{x}$	arithmetic mean	kN/m
x_{min}	smallest value of a threshold series	kN/m
$\bar{x}_n$	arithmetic mean for ln x	
x_o	probable threshold level	kN/m
α	altitude of the sun	rad
α	linear coefficient of thermal expansion	K^{-1}
α	parameter of Gumbel-distribution function	m/kN
$\bar{\alpha}$	weighted time average of part of source term depending on ambient conditions only	W/m^3
α_1	angle of incidence	rad
β	angle of refraction	rad
β	parameter of Gumbel - or exponential - distribution function	kN/m
β	weighting factor	-
γ	psycrometric "constant"	Pa/K
Δ	difference operator	-
Δx_x	ice growth during interval Δt	m
δ	declination of the sun	rad
ε	emissivity of the surface	-
ε	strain, deformation per unit length	-
ε_a	emissivity of the atmosphere	-
θ	temperature	^oC
θ_a	air temperature	^oC
$\bar{\theta}_i$	weighted time average of temperature for the i´th interval limit	^oC
θ_s	temperature of ice surface	^oC
λ	specific thermal conductivity	W/(mK)

λ	number of exceedances per year in average	-
μ	mean of x	kN/m
μ_n	mean of ln x	
ν	Poisson´s modulus	-
ρ	bulk density of snow or ice	kg/m^3
ρ_w	density of water	kg/m
σ	Stefan-Boltzmann´s constant	$W/(m^2k^4)$
σ	stress	Pa
σ_k	stress at point of time $t = k\Delta t$	Pa
σ	standard deviation for x	kN/m
σ_n	standard deviation for ln x	
φ	latitude	rad
χ^2	statistical test quantity	-
∂	differential operator	-
$\cdot$	$= \partial/\partial t$ first derivative with respect to time	-
$\cdot\cdot$	$=\partial^2/\partial t^2$ second derivative with respect to time	-
-	mean, time average, or weighted time average	-

LIST OF REFERENCES

Bergdahl, L. (1977): Physics of ice and snow as affects thermal pressure. Department of hydraulics, Chalmers University of Technology. Report Series A:1.

Bergdahl, L. (1978): Thermal Ice Pressure in Lake Ice Covers. Department of hydraulics, Chalmers University of Technology. Report Series A:2.

Flood Studies Report in Five Volumes. (1975): Volume I Hydrological Studies. Natural Environment Research Council. London 1975.

Gumbel, E.J. (1958): Statistics of Extremes. Columbia University Press, New York 1958.

Paily, P.P., Macagno, E.O. and Kennedy, J.F. (1974): Winter-Regime Surface Heat Loss from Heated Streams. IIHR Report No 155, Institute of Hydraulic Research, University of Iowa, Iowa City, Iowa, March 1974.

Taesler, R. (1972): Klimatdata för Sverige (Climate data for Sweden). National Swedish Council for Building Research, Stockholm 1972.

Institutionen för Vattenbyggnad

CHALMERS TEKNISKA HÖGSKOLA

Meddelanden

78. Cederwall, K.: Havet som recipient. Hydrodynamiska synpunkter.
Föredrag vid Sv. Havsforskningsföreningens årsmöte i Stockholm, mars 1975.

79. Sellgren, A.: Hydraulisk transport av fasta material i rör. 1975.

80. Andreasson, L. och Cederwall, K.: Rubbningar av grundvattenbalansen i urbana områden.
Hydrologisk konferens, Sarpsborg, 1975.

81. Cederwall, K.: Bräddning av avloppsvatten och effekten av utjämningsbassänger. "Världen, Vattnet och vi", Elmia 1975.

82. Cederwall, K.: Gross Parameter Solutions of Jets and Plumes. ASCE, HY5, May 1975.

83. Larsson, Sören och Lindquist, Per: Kalkning av försurade sjöar. Del I: Problembeskrivning samt utvärdering av kalkningen av Östra Nedsjön. Ex.arb. 1974:5.

84. Cederwall, K. och Svensson, T.: "Sediment flusing after dredging in tidal bays". 1975.

85. Göransson, C-G. och Svensson, T.: Strömkorsmätningar. Datorprogram för utvärdering inkl. korrektion för avdrift. Mars 1976.

86. Rahm, L. och Häggström, S.: Oskarshamns Kärnkraftverk. Modellstudier avseende kylvattenspridning vid framtida utbyggnad. Maj 1976. Del I Huvudrapport. Del II Bilagedel.

87. Sjöberg, A.: Beräkning av icke stationära flödesförlopp i reglerade vattendrag och dagvattensystem. Aug. 1976.

Slut på Meddelande-serien.

Institutionen för Vattenbyggnad

CHALMERS TEKNISKA HÖGSKOLA

Report Series A

A:1 Bergdahl, L.: Physics of ice and snow as affects thermal pressure. 1977

A:2 Bergdahl, L.: Thermal ice pressure in lake ice covers. 1978

Reports Series B

1. Bergdahl, L.: Beräkning av vågkrafter. 1977.

2. Arnell, V.: Studier av amerikansk dagvattenteknik. 1977.

3. Sellgren, A.: Hydraulic Hoisting of Crushed Ores. A feasibility study and pilot-plant investigation on coarse iron ore transportation by centrifugal pumps. 1977.

4. Ringesten, B.: Energi ur havsströmmar. 1977.

5. Sjöberg, A. och Asp, Th.: Brukar-anvisning för ROUTE-S. En matematisk modell för beräkning av icke-stationära flöden i floder och kanaler vid strömmande tillstånd. 1977.

6. Annual Report 76/77.

7. Bergdahl, L och Wernersson, L.: Calculated and Expected Thermal Ice Pressures in Five Swedish Lakes. 1977.

8. Göransson, C-G. och Svensson, T.: Drogue Tracking- Measuring Principles and Data Handling.

9. Göransson, C-G.: Mathematical Model of Sewage Discharge into confined, stratified Basins - Especially Fjords

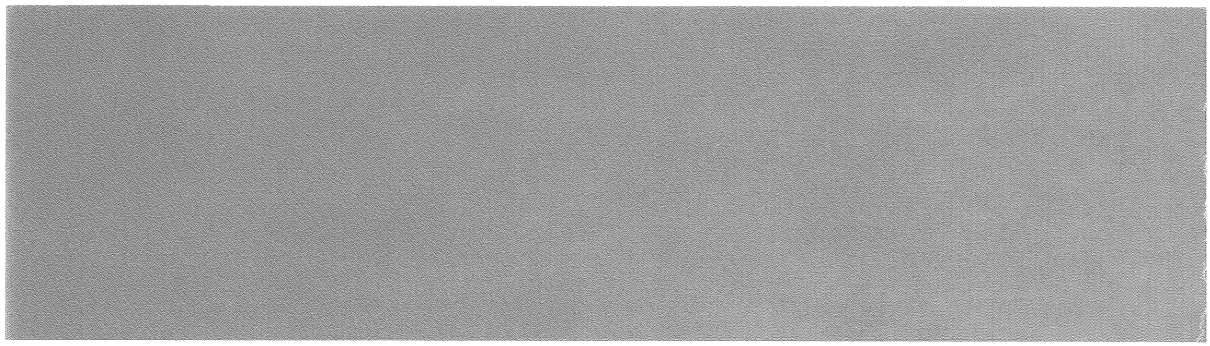

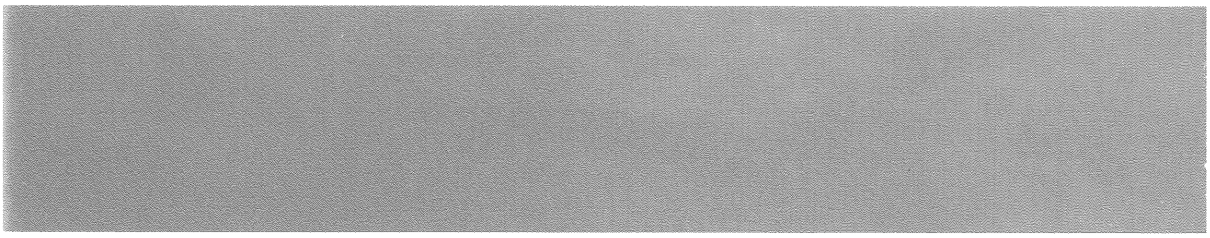

Printed in Sweden, Gotab, Kungälv, 1978.24687